



# Electrostatic Fields without Singularities: Theory, Algorithms and Error Analysis

MARCO PELLEGRINI

*Istituto di Matematica Computazionale del CNR, Pisa, Italy*

**Abstract.** The following problems that arise in the computation of electrostatic forces and in the Boundary Element Method are considered. Given two convex interior-disjoint polyhedra in 3-space endowed with a volume charge density which is a polynomial in the Cartesian coordinates of  $R^3$ , compute the Coulomb force acting on them. Given two interior-disjoint polygons in 3-space endowed with a surface charge density which is polynomial in the Cartesian coordinates of  $R^3$ , compute the normal component of the Coulomb force acting on them. For both problems adaptive Gaussian approximation algorithms are given, which, for  $n$  Gaussian points, in time  $O(n)$ , achieve absolute error  $O(c^{-\sqrt{n}})$  for a constant  $c > 1$ . Such a result improves upon previously known best asymptotic bounds. This result is achieved by blending techniques from integral geometry, computational geometry and numerical analysis. In particular, integral geometry is used in order to represent the forces as integrals whose kernel is free from singularities.

Categories and Subject Descriptors: F.2.2 [Analysis of Algorithms and Problem Complexity]: Nonnumerical Algorithms and Problems—*geometrical problems and computations*; G.1.4 [Numerical Analysis]: Quadrature and Numerical Differentiation—*error analysis*

General Terms: Algorithms, Theory

Additional Key Words and Phrases: Boundary elements method; electrostatic field

## 1. Introduction

1.1. THE PROBLEM. Coulomb's law states that a particle of charge  $q_1$  at position  $p_1$  exerts over a particle of charge  $q_2$  at position  $p_2$  a force  $\vec{F}_{12}$  given by:

$$\vec{F}_{12} = \frac{q_1 q_2}{4\pi\epsilon_0 |p_1 - p_2|^2} \frac{p_1 - p_2}{|p_1 - p_2|},$$

where  $\epsilon_0$  is the electric permeability of free space, and in the Gaussian unit system  $4\pi\epsilon_0 = 1$  [Jackson 1975]. Suppose now that we are given two fully

---

Part of this research has been done while visiting the International Computer Science Institute in Berkeley during August and September 1997.

Author's address: Istituto di Matematica Computazionale del CNR, Via S. Maria 46, 56126-Pisa, Italy, e-mail: pellegrini@imc.pi.cnr.it.

Permission to make digital/hard copy of part or all of this work for personal or classroom use is granted without fee provided that the copies are not made or distributed for profit or commercial advantage, the copyright notice, the title of the publication, and its date appear, and notice is given that copying is by permission of the Association for Computing Machinery (ACM), Inc. To copy otherwise, to republish, to post on servers, or to redistribute to lists, requires prior specific permission and/or a fee.

© 1999 ACM 0004-5411/99/1100-0924 \$5.00

dimensional convex bodies  $B_1$  and  $B_2$  endowed with volume charge density functions  $\rho_1$  and  $\rho_2$  respectively. We can formulate the total force acting on one of the two bodies by integrating Coulomb's law over the points of the two bodies:

$$\tilde{F}_{12} = \int_{p_1 \in B_1} \int_{p_2 \in B_2} \frac{\rho_1(p_1) dp_1 \rho_2(p_2) dp_2}{4\pi\epsilon_0 |p_1 - p_2|^2} \frac{p_1 - p_2}{|p_1 - p_2|}. \quad (1)$$

We will refer to integral (1) also as the volume-to-volume integral. If we are given two flat convex bodies  $P_1$  and  $P_2$  endowed with surface charge density functions  $\sigma_1$  and  $\sigma_2$ , the total force acting on one of the two bodies is given by the following integral:

$$\tilde{F}_{12} = \int_{p_1 \in P_1} \int_{p_2 \in P_2} \frac{\sigma_1(p_1) dp_1 \sigma_2(p_2) dp_2}{4\pi\epsilon_0 |p_1 - p_2|^2} \frac{p_1 - p_2}{|p_1 - p_2|}. \quad (2)$$

We will refer to integral (2) also as the surface-to-surface integral. This integral (2) has relevance in *direct* electrostatic problems, where the density of charge is known, however it is probably more useful in *inverse* electrostatic problems, where the actual distribution of charge is approximated by a truncated functional series. In such a case the density functions  $\sigma_1$  and  $\sigma_2$  in integral (2) are elements in the functional basis. Formula (1) can be seen as a generalization of (2). We obtain other integrals considered in the literature when we allow one of the two bodies to degenerate into a point (point-to-surface and point-to-volume integrals).

Analytic solutions of integral (1) and (2), or of similar integrals derived for the electrostatic potential, are rarely possible, or, whenever possible, might require complex and tedious symbolic calculations. Thus, often numerical integration is the method of choice. The main problem in a numerical evaluation of integrals (1) and (2) is that the kernel function is diverging within the integration domain when the closures of the bodies  $B_1$  and  $B_2$  (or the relative closures of  $P_1$  and  $P_2$ ) have points in common.

**1.2. OVERVIEW OF RESULTS IN THIS PAPER.** In this paper, we first manipulate integrals (1) and (2) with the objective of obtaining an equivalent formulation more suitable for numerical integration. Then we describe an approximation algorithm and we give the error analysis of the proposed algorithm. Before we give more details of the techniques used and the results obtained, we will briefly survey the current state of the art.

### 1.3. PREVIOUS WORK: NUMERICAL INTEGRATION

**1.3.1. Point-Singularity and Collocation Method.** Approximating an integral via the evaluations of the integrand function at selected points in the domain of integration is the classical problem of numerical integration [Davis and Rabinowitz 1975; Keast and Fairweather 1997; Espelid and Genz 1992]. The situation when the integrand function has singularities inside the domain of integration or on its boundary has been the subject of a substantial recent research effort (see, e.g., Duffy [1982], Lyness and Monegato [1980], Schwab [1994b], and a recent survey [Lyness and Cools, 1994]).

A problem often considered is when the domain is a simplex or a cube in  $d$ -dimensional space with a point singularity at a vertex (conventionally taken as the origin) [Duffy 1982; Lyness and Monegato 1980; Schwab 1994b]. Lyness [1976; 1978] and Lyness and Monegato [1980] show that for singularities of the form  $|p|^\alpha$ , where  $|p|$  the distance of a point  $p$  from the origin and  $\alpha$  a real number greater than  $-d$ , the error of a proposed recursive quadrature rule is expressed as an asymptotic expansion. Duffy [1982] showed that, for a class of singularities that includes the one described above, a certain variable transformation reduces the order of the singularity so that standard product integration rules may become applicable. Finally, for a vast class of functions with a singularity at the origin Schwab [1994b] proves that a proposed adaptive quadrature rule achieves an exponential error bound.

The theory in Lyness and Monegato [1980] and Schwab [1994b] does not seem to extend immediately to the case when the set of singularities has dimension two (e.g., two polyhedra sharing a face) or one (e.g., two triangles sharing an edge), which are the cases where integrals (1) and (2) have the worst singular behaviour. A straightforward application of the transformation proposed by Duffy does not produce immediately the desired softening of singularities on (1) and (2). However, if one of the two bodies degenerate into a point, then the point-to-surface or point-to-volume integral that is left from (1) and (2) fits in the framework of Duffy [1982], Lyness and Monegato [1980], Schwab [1994b]. This type of integrals with a point singularity are useful in the context of the Collocation method for the solution of integral equations of conductors [Zhou 1993]. An extensive treatment of singularities and quasi-singularities within the Collocation methods can be found in Schwab [1994a]. A heuristic method is described in Georg [1991].

*1.3.2. Integrals of the Galerkin Boundary Element Method.* Due to their importance for the boundary elements method (BEM for short) [Zhou 1993; Binns and Lawrenson 1973; Chiari and Silvester 1980] singular integrals similar to (2) have received special attention in the recent literature (see, e.g., Guermont [1992], Schwab and Wedland [1992a; 1992b]).

Hackbusch and Sauter [1993] consider a class of integrals which include integral (2) and obtain an equivalent formulation where the domain of integration is 3-dimensional and the kernel function has no singularities in the domain of integration. A tensor-product Gauss formula is used to evaluate the integral, however an error analysis of the proposed method is not given. Sauter and Schwab [1997] consider the same class of integrals and derive an equivalent formulation where the domain of integration is 4-dimensional and the kernel function does not diverge within the domain of integration. It is proved in Sauter and Schwab [1997] that the proposed tensor-product Gauss formula gives an error  $O(\exp(-b\sqrt[4]{n}))$  where  $n$  is the number of Gaussian points used by the algorithm, and  $b$  is a constant.

An issue related to the computation of integrals in the BEM is the structure of resulting stiffness matrix. The interplay between geometric meshing, approximation of the entries of the stiffness matrix, block structure of the matrix itself, and fast iterative solution methods is studied in von Petersdorff and Schwab [1996],

Hackbusch et al. [1995], and Sauter and Krapp [1996]. In this paper, we do not address such issue, which will be central in future research.

**1.4. FAST MULTIPOLE METHODS FOR POINT-TO-VOLUME INTEGRALS.** The fast multipole method [Rokhlin 1983] has found in recent years many applications to the solution of integral equations [Rokhlin 1983], to the  $n$ -body problem,<sup>1</sup> and in numerical integration of PDE [McKenney et al. 1995].

Mayo [1992] has proposed a method for evaluating volume integrals of potential theory by considering the equivalent Poisson equation. Such equation is then discretized using a finite difference approach. The weighted sum of the values of the potential field at nodal points within the domain of integration is used as final approximate value of the integral. This approach is greatly enhanced by the use of a fast Poisson solver such as those based on multipole expansions [McKenney et al. 1995; Greenbaum et al. 1993].

Integrals considered in Mayo [1992] are for the potential field (not the electrostatic field) and correspond to the case where one body degenerates into a point (point-to-volume integrals). However, the second body can have arbitrary shape as long as we have a routine to decide whether a nodal point is interior or exterior.

**1.5. A NEW APPROACH BASED ON INTEGRAL GEOMETRY.** The basic intuition behind the approach used in this paper is that electrostatic forces act along *straight lines* in a homogeneous medium, and moreover the module of Coulomb force is akin to one of the forms of the differential measure of lines in 3-space. As a consequence, it is possible to define the electrostatic force produced by extended bodies in 3-space as an integral over a set of lines in 3-space. Such a representation is independent of any coordinate system for lines. Afterwards, we choose a convenient way of representing lines in 3-space so to obtain for integral (1) a representation with a regular kernel. The theory developed for fully dimensional bodies is then used to support the derivation of a similar representation for the integral (2) relative to two flat bodies. We obtain integrals whose domain is the unit sphere of directions, while the value of the kernel at a given direction is associated to the orthogonal projection of the bodies  $B_1$  and  $B_2$  (respectively,  $P_1$ ,  $P_2$ ) in that direction. The new volume-to-volume and surface-to-surface integrals are approximated by a weighted sum of values of the kernel. The kernel is evaluated for a fixed direction by using techniques from computational geometry, while a finite set of directions is chosen with a Gaussian adaptive cubature rule. The main result of this paper is Corollary 1, which states that the value of integral (1) and the value of the normal component of integral (2) can be approximated in time  $O(n)$ , where  $n$  is the number of Gaussian points used, while achieving an error  $O(c^{-\sqrt{n}})$  for a constant  $c > 1$ .

**1.6. COMPARISON WITH PREVIOUS RESULTS: THEORETICAL ASPECTS.** Our result improves the error bound on approximating integral (2) from  $O(\exp(-\sqrt[4]{n}))$ , as in Sauter and Schwab [1997], to  $O(\exp(-\sqrt{n}))$ , where  $n$  is the number of Gaussian points used. However, the improved dependency on  $n$  has to be weighted against the possible increase in the time needed to compute the kernel

<sup>1</sup> See related work on the  $n$ -body problem in Appel [1985], Barnes and Hut [1986], Greengard [1988], Zhao [1987], Callahan and Kosaraju [1995], and Pan et al. [1992].

for each Gaussian point. This trade-off does not effect the asymptotic result but might impact on the actual running time for small values of  $n$ .

The theory in Sauter and Schwab [1997] and Hackbusch and Sauter [1993] applies to integral with singularities depending on a parameter that may assume a continuum of values, thus it has the potential for modeling a large class of phenomena. With our approach, we are able to treat singularities that can be interpreted geometrically. We could find such interpretation for integrals of the electrostatic field (this paper and Pellegrini [1996]), integrals of the potential field [Finocchiaro 1996] and integrals in radiosity [Pellegrini 1997]. At the moment, we do not have such an interpretation for, say, dipole integrals or those integrals arising in hypersingular integral equations.

As for the integral (1), representing the force between two extended bodies in 3-space, we could not find any method in literature with an error bound on its accuracy. As mentioned before, the method of Mayo [1992] computes the potential at a single point in space induced by a spatial charge distribution (point-to-volume).

A remarkable fact is that the theory, algorithms and error analysis we develop for the volume-to-volume case (integral (1)) is actually simpler than the equivalent for the surface-to-surface case (integral (2)). This is in sharp contrast with most methods where increase in dimension entails a more complex treatment. Sometimes 3-dimensional models are analyzed with the additional assumption that one dimension is much smaller than the others (thin-plate assumption) (see, e.g., Schwab [1995]); no such assumption is needed in our treatment.

Results in Hackbusch and Sauter [1993] and Sauter and Schwab [1997] are obtained using the concepts of *Cauchy principal value* and *Hadamard finite part integral* [Davis and Rabinowitz 1975; Hackbusch and Sauter 1993]. Intuitively, the method of the Cauchy principal value consists in choosing a subdomain  $D' \subset D$  of the integration domain  $D$  such that the singularity is in the difference  $D' \setminus D$ , then the limit of the integral over  $D'$  is taken, as  $D'$  tends to  $D$ . In the Hadamard finite part integral, besides the above described limiting process, the function itself is modified by subtracting the value of a Hölder continuous factor of the kernel, evaluated at the singular point. Our approach is rather different. We manipulate only the kernel function by using several formulations of the differential measure of lines. Uniqueness of geometric measures for lines ensures the equivalence of integrals based on different forms of the differential measure of lines. With this approach, we avoid completely limiting processes in the volume-to-volume integral. We still use limiting processes for the surface-to-surface case although not of the type described above.

**1.7. ORGANIZATION OF THE PAPER.** In Section 2, we derive a singularity-free form for the volume-to-volume integral (1). In Section 3, we derive a singularity-free form of the surface-to-surface integral (2) which arise naturally within the Boundary Element Method. Section 4 introduces the numerical integration scheme. In Section 5, we give the error analysis of the Gaussian adaptive integration algorithm for a class of *well-behaved* integrals. In Section 6, we describe a local systems of coordinates which is used in Sections 7 and 8 to prove that our geometric integrals are well-behaved so that the analysis in Section 5 holds for them. In Section 9, we report on experiments.

## 2. An Integral Geometric Theory of Electrostatic Fields

In this section, we present a geometric interpretation of electrostatic force fields using tools from integral geometry. We adopt an axiomatic approach. We give an integral geometric definition of a field  $\tilde{G}$ , which we will call the *geometric field*. We will show that the geometric field satisfies Gauss's Law of flux through a closed (convex) surface. Well-known arguments of electrostatics can then be invoked to base the classical theory of electrostatic fields on Gauss law [Jackson 1975; Landau and Lifshitz 1980]. The theory is developed for fully dimensional convex bodies in 3-space.

Let us denote with  $L$  an oriented line in 3 space, with  $\tilde{L}$  the unit vector along  $L$  and  $dL$  the differential measure of lines in 3-space. Let us consider a density function  $\rho_1(p)$  defined over the points  $p$  of a compact convex body  $B_1$ , and let  $\bar{\rho}_1$  be the maximum of the absolute value of  $\rho_1(p)$  in  $B_1$ . Let us define for a line  $L$  the quantity  $m_1(L)$ :

$$m_1(L) = \int_{p \in L} \rho_1(p) dp.$$

Notice that  $|m_1(L)| \leq \bar{\rho}_1 \mu(L \cap B_1)$ , where  $\mu$  measures the length of a segment, and equality holds for a constant density of charge. Let  $Q_1$  be the total charge of  $B_1$ :

$$Q_1 = \int_{p \in B_1} \rho_1(p) dp.$$

The Geometric field at a point  $p \notin B_1$  is defined as:

$$\tilde{G}_1(p) = \int_{L \cap p \neq \emptyset} m_1(L) \tilde{L} dL \quad (3)$$

The lines are considered oriented from  $B_1$  to  $p$ , and the integral is an integral of vectors. Since we consider convex bodies, although the lines are oriented, we use in many cases the underlying set of unoriented lines when it is convenient to do so. Sometimes, it is more convenient to work with the component of  $\tilde{G}$  in some direction  $\vec{w}$ , which is given by:

$$\tilde{G}_1 \cdot \vec{w} = \int_{L \cap p \neq \emptyset} m_i(L) (\tilde{L} \cdot \vec{w}) dL.$$

We will compare our results with those obtained through the traditional definition of the electrostatic field in the Gauss unit system (see Jackson [1975]).

**2.1. GAUSS LAW.** Gauss Law states that the integral of the component of the electric field  $\tilde{E}(p)$  in direction  $\vec{n}(p)$  normal to a closed connected surface  $S = \partial B$  is equal to  $4\pi$  times the total charge in the bounded connected region  $B$

enclosed by the surface  $S$ :

$$\int_{p \in S} \vec{E} \cdot \vec{n} dp = 4\pi \int_{p \in B} \rho(p) dp.$$

Let us take a convex surface  $S$  and let us parameterize the (directed) lines as a point on the surface and an (outer) direction  $u$  in the set of directions  $U/2$ . In these coordinates the differential element of lines is  $dL = \cos \theta dp du$ , where  $dp$  is the differential element of surface area,  $du$  is the differential element of directions, and  $\theta$  is the angle between the (outer) normal to  $\vec{n}(p)$  and the direction  $u$ . We have that:

$$\begin{aligned} \int_{L \cap S \neq \emptyset} m_1(L) dL &= \int_{p \in S} \int_{u \in U/2} m_i(L) \cos \theta du dp \\ &= \int_{p \in S} \vec{G}(p) \cdot \vec{n}(p) dp, \end{aligned}$$

where the last expression is the standard definition of the flux of a vector field through the surface  $S$ . Now we start from the same integral but we identify any line by a pair  $L = (u, q)$  where  $u$  is the direction of  $L$ , and  $q$  is the point intercepted by  $L$  on a plane  $P(u)$  of normal  $u$  and incident to the origin. Using these coordinates the differential measure of lines is  $dL = du \wedge dq$  [Santalo 1976]. Consider  $B_1 \subseteq B$ . We obtain:

$$\begin{aligned} \int_{L \cap S \neq \emptyset} m_1(L) dL &= \int_{L \cap B_1 \neq \emptyset} m_1(L) dL \\ &= \int_{u \in U} \left[ \int_q m_1(u, q) dq \right] du \\ &= \int_{u \in U} \left[ \int_q \left[ \int_{p \in L, L=L(u, q)} \rho_1(p) dp \right] dq \right] du \\ &= \int_{u \in U} \left[ \int_{p \in B_1} \rho_1(p) dp \right] du = 4\pi Q_1, \end{aligned}$$

where in the last integral the domain of  $q$  is the projection of  $B$  onto  $P(u)$ . To summarize, starting from the same integral we have derived two different expressions which we may therefore equate, obtaining:

$$\int_{p \in S} \vec{G}_1 \cdot \vec{n} dp = 4\pi Q_1,$$

which is the statement of Gauss's law for the field  $\vec{G}$ .

2.2. FORCE ACTING BETWEEN TWO CONVEX BODIES. From now on, we will not distinguish any more between the geometric field  $\vec{G}_i$  and the electrostatic field  $\vec{E}_i$  generated by a convex body  $B_i$ . Let us denote with  $\vec{F}_{12}$  the force acting between bodies  $B_1$  and  $B_2$ . We can express this force by integrating over the points of  $B_1$  the value of the electrostatic field generated by  $B_2$  at each such point. Formally, we have:

$$\vec{F}_{12} = \int_{p \in B_1} \vec{E}_2(p) \rho_1(p) dp,$$

which we expand using Formula (3) into:

$$\vec{F}_{12} = \int_{p \in B_1} \left[ \int_{L \cap p \neq \emptyset} m_2(L) \vec{L} dL \right] \rho_1(p) dp.$$

Now we transpose the two integrals obtaining:

$$\vec{F}_{12} = \int_L \int_L \left[ \int_{L \cap p \neq \emptyset, p \in B_1} m_2(L) \rho_1(p) dp \right] \vec{L} dL.$$

The function  $m_2(L)$  in the inner integral does not depend on  $p$ , thus we can take it out of the inner integral. The inner integral that is left is  $m_1(L)$ .

The total force acting between  $B_1$  and  $B_2$  is thus reduced to a single integral over the set of lines in 3-space:

$$\vec{F}_{12} = \int_L m_1(L) m_2(L) \vec{L} dL. \quad (4)$$

Now we identify any line by a pair  $L = (u, q)$  where  $u$  is the direction of  $L$ , and  $q$  is the point intercepted by  $L$  on a plane  $P(u)$  of normal  $u$  and incident to the origin. Using these coordinates the differential measure of lines is  $dL = du \wedge dq$  [Santaló 1976]. We obtain the new formula:

$$\vec{F}_{12} = \int_L m_1(L(u, q)) m_2(L(u, q)) \vec{u} dq du.$$

Thus, we can split the computation into an integration over the set  $U/2$  of unoriented directions,<sup>2</sup> and, for a fixed direction  $u \in U/2$ , an integration over a planar set of points. So finally:

$$\vec{F}_{12} = \int_{u \in U/2} V_{12}(u) \vec{u} du, \quad (5)$$

<sup>2</sup> The set of directions  $U$  is represented by the unit sphere in 3-space. We obtain the set of unoriented directions by identifying antipodal points on the unit sphere.



where the kernel function  $V_{12}$  is:

$$V_{12}(u) = \int_q m_1(L(u, q))m_2(L(u, q))dq. \quad (6)$$

*Remark.* The function  $V_{12}(u)$  does not diverge. This is a main advantage with respect to more traditional formulations of the force acting between two bodies that are based on integrating a kernel functions, such as  $1/r^2$  or  $1/r$ , which diverge when  $r$  goes to zero.

### 3. Integrals for the Boundary Element Method

To maintain the discussion self contained we show how to derive the BEM integral from Robin's integral equation for conducting bodies. Readers familiar with the Boundary Element Method may want to skip to Section 3.2.

**3.1. DISCRETIZATION OF THE ROBIN'S INTEGRAL EQUATION FOR CONDUCTING BODIES.** Robin's integral equation (7) describes the equilibrium conditions for the surface charge density  $\sigma(p)$  on the surface  $S = \partial D$  of a closed compact (but not necessarily connected) 3-dimensional domain  $D$  [Cade 1995]. In this section, we show a possible discretization of Robin's integral equation resulting in a Boundary Element formulation. We are interested in showing the typical form of the entries of the stiffness matrix. Then, in Section 3.2, we turn such entries into geometric integrals without singularities. Finally, we describe the algorithm for approximating such geometric integrals and we give the error analysis.

Robin's equation for the surface charge density function  $\sigma(p)$  over a surface  $S$  is the following:

$$2\pi\sigma(p) = \int_{p' \in S} \frac{\cos \theta(n(p), pp')}{r^2} \sigma(p') dp', \quad (7)$$

where  $\theta(n(p), pp')$  is the angle formed by the normal  $n(p)$  to  $S$  at  $p$  with the line  $p, p'$ , and  $r$  is the distance between  $p$  and  $p'$ . We now consider the surface as partitioned in polygons  $P_i$  with index  $i \in [1, \dots, k]$ , and we compute the force acting on each polygonal face  $P_i$ . Since the electric field is normal at any point of the polygon, and the normal direction to each polygon is constant, the resultant force is also normal to the polygon  $P_i$ . Let  $F_i$  be the modulus of the (normal) force acting on polygon  $P_i$ . We can compute  $F_i$  by using the well known relation  $E(p) = 2\pi\sigma(p)$  between the module of the field and the charge density at any point of the surface  $S$ . With  $\sigma_i$  we denote the restriction of the function  $\sigma$  on  $P_i$ . We obtain:

$$F_i = \int_{p \in S} E_i(p) \sigma_i(p) dp = \int_{p \in S} 2\pi\sigma_i(p) \sigma_i(p) dp. \quad (8)$$

If we use the right side of the Eq. (7), we obtain:

$$F_i = \int_{p \in S} E_i(p) \sigma_i(p) dp \quad (9)$$

$$= \int_{p \in S} \left[ \sum_{j=1, i \neq j}^k \int_{p' \in S_j} \frac{\cos \theta(n(p), pp')}{r^2} \sigma_j(p') dp' \right] \sigma_i(p) dp. \quad (10)$$

Now we expand each local density function  $\sigma_i$  in an orthonormal basis with unknown scalar coefficients  $A_{i,h}$ :

$$\sigma_i(p) = A_{i,0} \sigma_0(p) + A_{i,1} \sigma_1(p) + A_{i,2} \sigma_2(p) + \dots$$

Denoting with  $H_{i,h}$  the following integral:

$$H_{i,h} = 2\pi \int_{p \in P_i} \sigma_h(p) \sigma_h(p) dp,$$

and exploiting orthonormality<sup>3</sup> we obtain that formula (8) for  $F_i$  becomes:

$$F_i = H_{i,0}[A_{i,0}]^2 + H_{i,1}[A_{i,1}]^2 + H_{i,2}[A_{i,2}]^2 + H_{i,3}[A_{i,3}]^2 + \dots$$

Expanding formula (9) for  $F_i$  we obtain:

$$F_i = \sum_j \sum_h \sum_k \int_{p \in S_i, p' \in S_j} \frac{\cos \theta(n(p), pp')}{r^2} \sigma_h(p) \sigma_k(p') A_{i,h} A_{j,k} dp dp'.$$

The above identities are satisfied by the solution of this system:

$$H_{i,h} A_{i,h} = \sum_j \sum_k A_{j,k} \int_{p \in S_i, p' \in S_j} \frac{\cos \theta(n(p), pp')}{r^2} \sigma_h(p) \sigma_k(p') dp dp'.$$

The unknowns in the resulting linear system are the values of  $A_{i,h}$ . The number of such variables, sometimes referred to as the “dimension” of the system, is the product of the number of polygons  $P_i$  and the number of terms of the expansion of the density functions, in case of a uniform expansion on all the patches (also known as h-Galerkin method). Alternatively we might truncate the basis expansions differently on each polygon  $P_i$  so the total number of unknown is the sum of the terms in the truncated functional expansions (also known as hp-Galerkin). The coefficients  $H_{i,h}$  can be precomputed easily with exact analytic integration. The other coefficients on the right sides of the equations are of the form:

$$C_{i,h,j,k} = \int_{p \in S_i, p' \in S_j} \frac{\cos \theta(n(p), pp')}{r^2} \sigma_h(p) \sigma_k(p') dp dp', \quad (11)$$

<sup>3</sup> The integral of product of functions with different index is null.

where the functions  $\sigma_h$  and  $\sigma_k$  are known elements of the functional basis. Next we show how we can compute such coefficients using the general techniques developed in the first part of the paper. Integrals of this form (11) fall within the class of integrals studied in Sauter and Schwab [1997]. They are obtained in that paper with a double-layer potential formulation of the equilibrium of conductors.

**3.2. INTEGRAL GEOMETRIC TRANSFORMATION.** In this section, we apply integral geometric transformations to the integral in (11). To simplify the notation we drop subscripts inherited from the discretization process and we consider two triangles  $T_1$  and  $T_2$  and known densities  $\sigma_1$  and  $\sigma_2$ . Thus, the integral we are considering is:

$$C_{12} = \int_{p \in T_1, p' \in T_2} \frac{\cos \theta(n(p), pp')}{r^2} \sigma_1(p) \sigma_2(p') dp dp' \quad (12)$$

Let us call  $\phi(n(p'), pp')$  the angle formed by the line  $pp'$  with the normal to  $T_2$  at  $p'$ . Let us assume for the moment being that the cosine of such angle is not null. Multiplying and dividing in (11) by the cosine of this angle we obtain:

$$\int_{p \in T_1, p' \in T_2} \frac{1}{\cos \phi(n(p'), pp')} \frac{\cos \theta(n(p), pp') \cos \phi(n(p'), pp')}{r^2} \sigma_1(p) \sigma_2(p') dp dp'.$$

Now we can turn to a geometric integral since we have isolated an expression of  $dL$ :

$$\int_{L, L \cap T_1 \neq \emptyset, L \cap T_2 \neq \emptyset} \frac{1}{\cos \phi(n(p'), p, p')} \sigma_1(p) \sigma_2(p') dL. \quad (13)$$

Next we express a line  $L$  in the  $(u, q)$  coordinates;

$$\int_{u \in U} \left[ \int_q \frac{1}{\cos \phi(q, u)} \sigma_1(p) \sigma_2(p') dq \right] du.$$

For flat polygonal faces and a fixed direction  $u$  the value  $\cos \phi(q, u)$  does not depend on  $q$  and can be taken out of the inner integral sign:

$$C_{12} = \int_{u \in U} \left[ \frac{1}{\cos \phi(u)} \int_q \sigma_1(p) \sigma_2(p') dq \right] du. \quad (14)$$

Let us call  $K'(u)$  the kernel integral:

$$K'(u) = \frac{1}{\cos \phi(u)} \int_q \sigma_1(p) \sigma_2(p') dq. \quad (15)$$

In the next sections, we will show that the value of  $K'(u)$  does not diverge for  $\cos \phi(q, u)$  going to zero and that the value of the limit can be computed with a formula obtained by a limiting process starting from formula (5).

*Remark.* We can obtain formula (13) by considering the formula (5) in the first part of the paper applied to two prisms with basis  $T_1$  and  $T_2$  and by letting the height of the prisms go to zero while maintaining a consistency condition on the local charge.

LEMMA 1. *The function  $K'(u)$  is bounded, for every  $u \in U$  where it is defined.*

PROOF. Densities  $\sigma_1$  and  $\sigma_2$  are polynomials over bounded domains, therefore they have a well-defined absolute maximum which we denote  $\bar{\sigma}_1$  and  $\bar{\sigma}_2$ . Let  $A'_{12}$  be the area of the intersection of the projections of  $T_1$  and  $T_2$  onto a plane of normal  $u$ . An upper bound for  $K'(u)$  is:

$$K'(u) \leq \bar{\sigma}_1 \bar{\sigma}_2 \left( \frac{1}{\cos \phi} \right) A'_{12}$$

Now for a generic direction  $u$  with  $\cos \phi \neq 0$  we have

$$\frac{1}{\cos \phi} = \frac{A_2}{A'_2},$$

where  $A_2$  is the area of  $T_2$  and  $A'_2$  is the area of the projection of  $T_2$  onto a plane of normal  $u$ . Since always  $A'_{12} \leq A'_2$ , we have that the expression

$$\frac{A_2}{A'_2} A'_{12}$$

is bounded by  $A_2$  which is a finite value independent of  $u$ .  $\square$

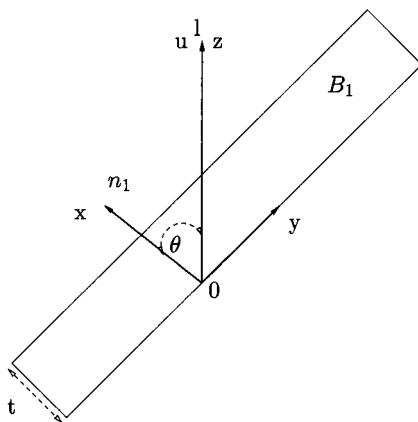
From Lemma 1, we know that  $K'(u)$  is bounded for every direction  $u$  for which it is defined. We obtain a real analytic extension in directions  $u$  for which  $K'(u)$  is not defined by taking an extension that coincides with the limit of  $K'(u)$ . In this section, we derive a precise formula for such limit function  $K''(u)$  by applying a limit process to the theory of the electrostatic force of extended bodies in Section 2. We show the following theorem:

THEOREM 1. *The entry  $C_{12}$  in the stiffness matrix defined in (11) is given by:*

$$C_{12} = \int_{u \in U} K(u) du. \quad (16)$$

where,

$$K(u) = \begin{cases} K'(u) & \text{if } \cos \theta(u) \neq 0 \text{ and } \cos \phi(u) \neq 0, \\ K''(u) & \text{if } \cos \theta(u) \neq 0 \text{ and } \cos \phi(u) = 0, \\ 0 & \text{if } \cos \theta(u) = 0. \end{cases} \quad (17)$$

FIG. 1. Geometric setting for  $B_1$ : cross-section at  $\eta = 0$ .

PROOF. When  $\cos \theta(u) = 0$  the contribution of direction  $u$  to the integral (16) is null since such integral represents the normal component of the force. When  $\cos \theta(u) \neq 0$  and  $\cos \phi(u) \neq 0$  the derivation of Section 3.2 is valid and gives the value of the kernel  $K'(u)$ , as defined in (15). Finally we have shown that  $K'(u)$  is always bounded so we can take its limit value  $K''(u)$  of  $K'(u)$  for  $\cos \phi(u) \rightarrow 0$  as the real analytic extension of kernel.  $\square$

3.3. REAL ANALYTIC EXTENSION OF THE KERNEL. In this section, we derive formula (19) that is a representation of  $K''(u)$  useful for the algorithm and the error analysis.

We consider two prisms. Prism  $B_1$  (respectively,  $B_2$ ) has basis  $T_1$  (respectively,  $T_2$ ) and height  $t$ . We associate the surface charge density  $\sigma_1$  (respectively,  $\sigma_2$ ) to the basis and the volume charge density  $\rho_1$  (respectively,  $\rho_2$ ) to the prisms according to a rule to be specified later. We consider a direction  $u$  such that  $\cos \theta(u) \neq 0$  and  $\cos \phi(u) = 0$ .

*Geometric setting for  $B_1$ .* Let  $l$  be a line in direction  $u$ . The reference frame and coordinates relative to body  $B_1$  are as follows: Let  $\theta$  be the angle of  $l$  with the normal  $n_1$  to  $T_1$ , let  $z$  be the coordinate of points on  $l \cap B_1$  taking as zero the entry point of the line  $l$  in  $B_1$ . Let  $x$  be the coordinate on the normal direction  $\vec{n}_1$  and let  $y$  the coordinate along the surface  $T_1$  on the plane defined by  $l$  and  $\vec{n}_1$ . Let  $\eta$  be the coordinate on an axis orthogonal to  $l$  and  $n_1$ . In Figure 1, the cross section of  $B_1$  at  $\eta = 0$  is shown.

The following relations hold among the several coordinates relative to the same point on  $l$ :  $y = x(\tan \theta)$ ,  $z = x/(\cos \theta)$ , and consequently:  $y = z(\sin \theta)$ . The ranges are:  $0 \leq x \leq t$ ,  $0 \leq y \leq t(\tan \theta)$ ,  $0 \leq z \leq t/(\cos \theta)$ . We set the following relation among surface charge density and volume charge density:  $\rho(z) = \sigma(y)/t$ .

*Contribution of  $B_1$  along line  $l$ .* Now we give an explicit formula for the weight of  $l$  in  $B_1$  which is given by:

$$m_1(l) = \int_{z=0}^{t/(\cos \theta)} \rho(z) dz$$

We make a change of variable in the integral. Since  $dy/(\sin \theta) = dz$ , we obtain:

$$m_1(l) = \int_{y=0}^{t(\tan \theta)} \left( \frac{\sigma(y)}{t} \right) \left( \frac{dy}{(\sin \theta)} \right) = \frac{1}{(t \sin \theta)} \int_{y=0}^{t(\tan \theta)} \sigma(y) dy$$

Now we expand the  $\sigma_1$  function in a series of McLaurin at the origin, assuming the appropriate differentiability conditions, which are satisfied by polynomials.

$$m_1(l) = \frac{1}{(t \sin \theta)} \int_{y=0}^{t(\tan \theta)} \left[ \sigma(0) + y \left( \frac{d\sigma}{dy} \right)_0 + \cdots \right] dy$$

Integrating each term separately:

$$m_1(l) = \frac{1}{(t \sin \theta)} \left[ y\sigma(0) + \frac{y^2}{2} \left( \frac{d\sigma}{dy} \right)_0 + \cdots \right]_{y=0}^{t(\tan \theta)}.$$

We obtain:

$$m_1(l) = \frac{1}{(t \sin \theta)} \left[ t(\tan \theta)\sigma(0) + \left( \frac{1}{2} \right) t^2(\tan \theta)^2 \left( \frac{d\sigma}{dy} \right)_0 + \cdots \right].$$

Letting  $t$  go to zero only the first term remains:

$$m_1(l) = \frac{\sigma(0)}{\cos \theta},$$

where  $\sigma(0)$  is the density of charge at the point where  $l$  meets  $S_1$ .

*Geometric setting for  $B_2$ .* Now we consider the weight of the line  $l$  with respect to the second slab with normal  $\tilde{n}_2$  orthogonal to the direction  $u$ . Let us consider for  $B_2$  a coordinate  $z$  on  $l$ . Notice that now  $l$  forms an angle of  $\pi/2$  with the normal  $n_2$  to  $T_2$ .

We take a coordinate  $\xi$  on an axis parallel to  $n_2$ , and a coordinate  $\eta$  in a direction that forms an orthogonal triple with  $u$  and  $\tilde{n}_2$ . In Figure 2, the cross section of  $B_2$  at  $\eta = 0$  is shown. To keep calculations simple, we show first what happens in plane  $\eta = \text{const}$ , then we will integrate the formula obtained in  $d\eta$  within the relevant range of values of  $\eta$  to obtain the final result. We consider the  $\eta$  coordinate fixed and we work for the moment only with the  $\xi$  and  $z$  coordinates. The limits are:  $0 \leq \xi \leq t$ ,  $Z_{1\eta} \leq z \leq Z_{2\eta}$ .

*Contribution of  $B_2$  along line  $l$ .* Now we compute the weight of a line  $l$  parallel to  $u$ :

$$m_2(l) = \int_{z=Z_{1\eta}}^{Z_{2\eta}} \rho_2(z, \xi) dz = \int_{z=Z_{1\eta}}^{Z_{2\eta}} \frac{\sigma_2(z)}{t} dz = \left( \frac{1}{t} \right) \int_{z=Z_{1\eta}}^{Z_{2\eta}} \sigma_2(z) dz = \left( \frac{1}{t} \right) M_\eta,$$

where we have denoted with  $M_\eta$  the integral

$$M_\eta = \int_{z=Z_{1\eta}}^{Z_{2\eta}} \sigma_2(z) dz. \quad (18)$$

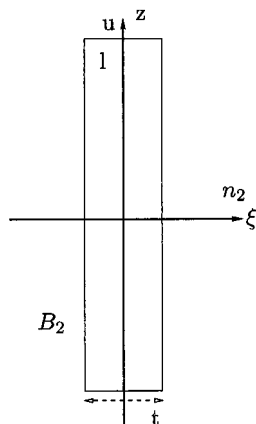


FIG. 2. Geometric setting for  $B_2$ : cross-section at  $\eta = 0$ .

Since both the integration limits and the integrand are polynomials for a fixed direction  $u$ , a closed-form representation of the integral  $M_\eta$ , it is not difficult, although tedious, to derive.

*Application of formula (5).* Formula (11) represents the normal component with respect to  $T_1$  of the force acting between  $T_1$  and  $T_2$  endowed with charge densities  $\sigma_1$  and  $\sigma_2$ . Thus, we can express the normal component of such a force using formula (5) of the first part of the paper:

$$\begin{aligned} C_{12} &= \lim_{t \rightarrow 0} (\vec{n}_1 \cdot \vec{F}_{12}) \\ &= \lim_{t \rightarrow 0} \int_{u \in U} \cos \theta \left[ \int_q m_1 m_2 dq \right] du. \end{aligned}$$

We can now specialize this formula for the prisms  $B_1$  and  $B_2$  using the quantities precomputed above we have:

$$\int_u \cos \theta \left[ \int_\eta \int_\xi \left( \frac{\sigma_1(\xi, \eta)}{\cos \theta} \right) \left( \frac{1}{t} \right) M_\eta d\xi d\eta \right] du.$$

Let us perform the simplification of the cosines and consider the innermost integral, apply McLaurin expansion and let  $t$  tend to zero.

$$\begin{aligned} &\int_{\xi=0}^t \sigma_{1,\eta}(\xi) (1/t) M_\eta d\xi \\ &= M_\eta \left( \frac{1}{t} \right) \int_{\xi=0}^t \left[ \sigma(0) + \xi \left( \frac{d\sigma(\xi)}{d\xi} \right)_0 + \dots \right] d\xi \end{aligned}$$

$$\begin{aligned}
&= M_\eta \left( \frac{1}{t} \right) \left[ \xi \sigma(0) + \xi^2 \left( \frac{1}{2} \right) \left( \frac{d\sigma(\xi)}{d\xi} \right)_0 + \cdots \right]_{\xi=0}^t \\
&= M_\eta \sigma_{1,\eta}(0).
\end{aligned}$$

So we obtain a final integral:

$$\int_u \left[ \int_\eta M_\eta \sigma_\eta d\eta \right] du$$

Thus, the kernel is:

$$\int_\eta M_\eta \sigma_\eta d\eta = K''(u) \quad (19)$$

*Remark.* Note that  $K''(u)$  is an integral on a one-dimensional domain, while  $K'(u)$  is an integral over a two dimensional domain.

*Remark.* The formula we obtain for the case  $\cos \phi = 0$  has been obtained under the condition that  $\cos \theta \neq 0$ . On the other hand, the final formula does not contain any diverging function of  $\cos \theta$  so there are no numerical issues in evaluating such a formula also for directions  $u$  for which  $\cos \theta = 0$ . What we need to make sure is that the value obtained by the formulae of the kernel tends to zero. This is the case for  $K'(u)$  since this is an area integral and, when  $\cos \theta = 0$  the domain is at most 1-dimensional. This is also the case for  $K''(u)$  since when both  $\cos \theta = 0$  and  $\cos \phi = 0$  the domain of integration is zero dimensional (a point) for noncoplanar polygons so the integral defined by  $K''(u)$  tends to zero.

#### 4. Numerical Integration

In the first part of the paper (Sections 2 and 3), we have shown that some classical integrals of electrostatics can be represented in an integral geometric form (5) and (16) in such a way that the kernel functions (6) and (17) do not diverge and can be evaluated exactly. Both integrals have been reduced to an integral on the unit sphere of directions. The next step is to set up a scheme for the numerical approximation of such integrals.

Approximating an integral via a weighted sum of values of the integrand function at selected points in the domain of integration is the classical problem in numerical integration [Davis and Rabinowitz 1975]. Several basic techniques are available for low dimensional domains (see a recent survey by Cools [1997]). We will mention three techniques: Monte Carlo, Quasi Monte Carlo, and Gaussian quadrature.

In numerical integration, the integral  $\int_D f(x)dx$  is approximated by the summation  $\sum_i w_i f(x_i)$  where the discrete set of points  $x_i$ , for  $i = [1, N]$  is a subset of the domain  $D$ . If we use on  $U$  coordinates  $u = (\alpha, \beta)$ , then we will have a differential measure  $du = g(\alpha, \beta)d\alpha d\beta$ , and the domain  $D$  is the image of  $U$  onto  $R^2$  given by the coordinate system. The function  $f$  is thus the product



of  $g(\alpha, \beta)$  and the geometric kernel (e.g.,  $K(u)$  for BEM integrals or  $V_{12}(u)(u \cdot w)$  for the component of the force between tetrahedra in direction  $w$ ).

*Monte Carlo approach.* The points  $u_i = (\alpha_i, \beta_i)$  are chosen uniformly at random in  $D$ . The weights are all equal to  $|D|/N$ . See Pellegrini [1996] for an application of Monte Carlo integration to integral (5).

Monte Carlo error bounds have a typical error bound  $O(N^{-1/2})$ , provided the variance of the integrand function is bounded. A bound of this form has been proved in Pellegrini [1996].

*Quasi Monte Carlo approach.* The points  $u_i = (\alpha_i, \beta_i)$  are chosen in  $D$  so to have low discrepancy [Niederreiter 1992]. The weights are all equal to  $|D|/N$ . See Bientinesi and Pellegrini [1997] for an application of Quasi Monte Carlo to the integral (5).

Quasi Monte Carlo error bounds have a typical error bound roughly  $O(N^{-1})$  provided the total variation of the integrand function is bounded.

*Gaussian quadrature and cubature formulas.* The points  $u_i = (\alpha_i, \beta_i)$  are chosen in  $D$  by an appropriate scaling of the zeroes of Legendre polynomials [Davis and Rabinowitz 1975]. The weights are also derived from operations on the Legendre polynomials. We have a Gaussian quadrature rule (for dimension 1) of degree  $n$  when we choose points  $x_i$  and weights  $w_i$  so to give zero error on univariate polynomials up to degree  $2n - 1$ .

In the second part of the paper (Sections 4.1, 5, and 6), we describe an adaptive cubature Gaussian algorithm for evaluating (5) and (16) with error  $O(c^{-\sqrt{N}})$  for a constant  $c > 1$ .

**4.1. ADAPTIVE GAUSSIAN CUBATURE ALGORITHM.** We shall first describe the algorithm for approximating BEM integral (16). In Section 8, we shall derive the algorithm for integral (5) and its analysis.

The main idea is to study the kernel function  $K(u)$  so to isolate regions of the unit sphere  $U$  where  $K(u)$  is determined by a combinatorially fixed set of geometric features of the input triangles. Then each such region is refined into sub-domains so to obtain (i) a good parameterization of the integration subdomain, and (ii) good smoothness properties of the integrand function.

First, we show how we derive the exponential error bound from well established theorems in numerical integration, provided that some properties hold for the problem at hand. Secondly we prove that such properties actually hold. The description of the algorithm is carried out together with its error analysis.

## 5. Error Analysis

**5.1. FROM TWO DIMENSIONS TO ONE DIMENSION.** We relate the error of a quadrature product Gauss rule to the error in the evaluation of restrictions of the function by 1-dimensional Gauss quadrature rule. Here we borrow Proposition 6 and 7 (pages 23–26) from von Petersdorff and Schwab [1996] (see also Stroud [1971], pages 137–148). Note however that, in von Petersdorff and Schwab [1996], the space of integration is four-dimensional while here it is two-dimensional.

**LEMMA 2.** *Let  $f(x, y)$  be a continuous function of two variables with  $x \in [-a, +b] = \Omega_1$ ,  $y \in [-c, +d] = \Omega_2$ . Let  $\mathcal{I}_1$  be the integral operator on the first*

variable,  $\mathcal{I}_2$  the integral operator on the second variable and  $\mathcal{I}$  the bidimensional integral operator. Let

$$\mathcal{I}f = \mathcal{I}_1\mathcal{I}_2f = \int_{\Omega_1} \int_{\Omega_2} f(x, y) dx dy.$$

Let  $Q_1$  be a quadrature rule for  $\Omega_1$  and  $Q_2$  a quadrature rule for  $\Omega_2$ ,  $\mathcal{E}$  the error operator, then:

$$\begin{aligned} |\mathcal{E}f| &= |(\mathcal{I}f - Q_1Q_2f)| \\ &\leq |\Omega_1|(\max_{x \in \Omega_1} |(\mathcal{I}_2 - Q_2)f_x(y)|) + |\Omega_2|(\max_{y \in \Omega_2} |(\mathcal{I}_1 - Q_1)f_y(x)|), \end{aligned}$$

where  $f_x(y)$  and  $f_y(x)$  are restrictions of  $f(x, y)$  on the first and second variable.

PROOF. See Proposition 6 in von Petersdorff and Schwab [1996].  $\square$

**5.2. GAUSSIAN ERROR IN ONE DIMENSION.** We shall use the following result of Davis and Rabinowitz [1975] that relate the error of a Gaussian quadrature rule to the size of the region where the integrand function has an analytic extension in the complex plane (Formula 4.6.1.11 in Davis and Rabinowitz [1975], page 312, also Proposition 5 in von Petersdorff and Schwab [1996]):

**LEMMA 3.** *Let  $f(x)$  be real analytic in  $[-1, 1]$  and admit an analytic continuation  $f(z)$  with  $z = x + iy$  in the complex plane within a closed ellipse  $\mathcal{G}$  with foci at  $+1, -1$  and semi-axis sum  $\gamma$ , then:*

$$|\mathcal{E}(f)| = |\mathcal{I}f - Q_nf| \leq c \gamma^{-2n} \max_{z \in \partial \mathcal{G}} |f(z)|$$

where  $\mathcal{I}f = \int_{-1}^1 f(x) dx$  and  $Q_nf$  is the  $n$ -points Gaussian quadrature rule.

**5.3. WELL-BEHAVED INTEGRALS.** This concept provides the link between the general error bounding lemmas of the previous sections and the BEM-integrals we consider.

**Definition 1.** Integral

$$\int_{u \in U} f(u) du$$

is well behaved if it can be represented as

$$\sum_j \int_{u \in D_j} f_j(u) du,$$

where for each  $j$ ,  $D_j \subset U$ ; and for each  $j$  we can find a local system of reference  $LSR_j$  of parameters  $\alpha_j$  and  $\beta_j$  such that

(1) In  $LSR_j$ ,

$$D_j = I_{j,\alpha} \times I_{j,\beta} = [\alpha_{j,0}, \alpha_{j,1}] \times [\beta_{j,0}, \beta_{j,1}]$$

That is,  $D_j$  is mapped to a bounded rectangular domain in  $LSR_j$ .

- (2) By substitution  $f_j(u)$  is mapped to  $f_j(\alpha_j, \beta_j)$  and we have the invariant differential element of directions  $du = g_j(\alpha_j, \beta_j) d\alpha_j d\beta_j$ .
- (3) For every  $\bar{\alpha} \in I_{j,\alpha}$ , the restriction  $f_j(\bar{\alpha}, \beta_j) g_j(\bar{\alpha}, \beta_j) : I_{j,\beta} \rightarrow R$  admits an analytic extension in an open rectangle  $Rect(\bar{\alpha})$  of the complex plane that contains strictly  $I_{j,\beta}$ .
- (4) For every  $\bar{\beta} \in I_{j,\beta}$ , the restriction  $f_j(\alpha_j, \bar{\beta}) g_j(\alpha_j, \bar{\beta}) : I_{j,\alpha} \rightarrow R$  admits an analytic extension in an open rectangle  $Rect(\bar{\beta})$  of the complex plane that contains strictly  $I_{j,\alpha}$ .

By set  $A$  strictly containing  $B$  we mean that  $A$  contains  $B$  and the boundary of  $A$  is disjoint from the boundary of  $B$ .

The following two lemmas are central in the proof of the error bound:

LEMMA 4. *Integral (16) is well behaved.*

PROOF. Discussion in Section 6 constitutes the proof of this lemma.

LEMMA 5. *Integral (5) is well behaved.*

PROOF. Discussion in Section 6 together with the modifications and simplifications in Section 8 constitutes the proof of this lemma.

5.4. PUTTING THINGS TOGETHER. Lemmas 2, 3, and 1 imply the following result:

THEOREM 2. *A well-behaved integral can be approximated using  $O(n)$  Gaussian point while achieving error  $O(c^{-\sqrt{n}})$  for some  $c > 1$ .*

PROOF. It is sufficient to prove the exponential bound for each  $D_j$  separately, since the number of such regions is independent of the number of Gaussian points used, and is bounded by a (small) constant. We drop the subscript  $j$  for the rest of this section. We consider for each  $\bar{\alpha}$  the rectangle  $Rect(\bar{\alpha})$  and we shift and scale it so that the included interval  $I_\beta$  coincides with the interval  $[-1, 1]$ . Let us call the scaled rectangle  $ScRect(\bar{\alpha})$ . Consider the intersection of all the scaled rectangles for all  $\bar{\alpha} \in I_\alpha$ :

$$IntScRect_\alpha = \bigcap_{\bar{\alpha} \in I_\alpha} ScRect(\bar{\alpha}).$$

Such a rectangle  $IntScRect_\alpha$  contains strictly the real closed interval  $[-1, 1]$ , therefore we can find an ellipse of semi-axis sum  $c > 1$  which strictly contains  $[-1, 1]$  and is strictly contained in  $IntScRect_\alpha$ . Therefore, the value of the function  $f$  on the boundary of the ellipse is bounded. Let us call  $M$  the maximum of the function on the boundary of the ellipse. Plugging  $M$  and  $c$  in Lemma 3, we obtain a bound on the error of computing the Gaussian approximation of the integral of a  $\alpha$ -restriction of  $f$ . Since this bound holds for every  $\bar{\alpha}$ , it is also a bound on the maximum error of an  $\alpha$ -restriction. Such a bound multiplied by  $|\beta_0 - \beta_1|$  gives the first term of the error in Lemma 2. A symmetric argument is

used for the second error term in Lemma 2. This concludes the proof of the theorem.  $\square$

From Theorem 2, Lemma 4 and Lemma 5, it follows

**COROLLARY 1.** *Integrals (5) and (16) can be approximated using  $O(n)$  Gaussian point while achieving error  $O(c^{-\sqrt{n}})$  for some  $c > 1$ .*

## 6. Domain Decomposition and Choice of Coordinates

In this section, we show a specific choice of coordinates in which we express the geometric entities of the first part of the paper. We thus establish the property point (1) for the subdomains of a well-behaved integral. We give a specific form to the differential measure on the unit sphere (point (2)). Moreover, we prepare the setting for the proof of property (3) and (4) to be carried out in Section 7.

**6.1. ON THE VERTICES OF THE INTEGRATION DOMAIN.** Let us call  $(x, y, z)$  the coordinates of a point  $p$  in an absolute Cartesian reference system. And let  $q = (X, Y)$  represent the coordinates of the point on a plane  $P(u)$  of normal direction  $u$ . Consider the formula for the BEM integral:

$$C_{12} = \int_{u \in U/2} \left[ \frac{1}{\cos \phi} \int_q \sigma_1(q) \sigma_2(q) dq \right] du.$$

Let  $T_1$  and  $T_2$  be triangles in 3-space,  $U$  the sphere of directions,  $U/2$  the sphere of directions with identified opposite directions. With  $T_i(u)$  we denote the projection of  $T_i$  onto the plane  $P(u)$ . Let  $\sigma_1(x, y, z(x, y))$  be the density function associated with triangle  $T_1$ , and  $\sigma_2(x, y, z(x, y))$  be function associated with triangle  $T_2$ . We consider the image of such functions on the plane  $XY$ , given by:  $f_i = \sigma_i(x(X, Y), y(X, Y), z(x(X, Y), y(X, Y))) = f_i(X, Y)$ ,  $i \in \{1, 2\}$ . Thus, the function we want to integrate in the inner integral is  $f_{12}(X, Y) = f_1(X, Y) f_2(X, Y)$ . The domain of integration is the set  $T_1(u) \cap T_2(u)$ , which is a convex polygon on  $P(u)$ . Let us call  $Vert(u) = \{(X_0, Y_0), \dots, (X_k, Y_k)\}$  the collection of its vertices in counterclockwise order.

**LEMMA 6.** *The integral*

$$A_{12}(u) = \int_q \sigma_1(q) \sigma_2(q) dq \tag{20}$$

*is expressible as a polynomial in the coordinates of points in  $Vert(u)$  in the  $XY$  local reference system.*

**PROOF.** The objective is to express the inner integral as a function of the coordinates of points in  $Vert(u)$ . We use Green's formula on the plane stating that, for functions  $h$  and  $k$

$$\int_D \left( \frac{\partial h}{\partial x} - \frac{\partial k}{\partial y} \right) dx dy = \int_{\partial D} k dx + h dy. \tag{21}$$

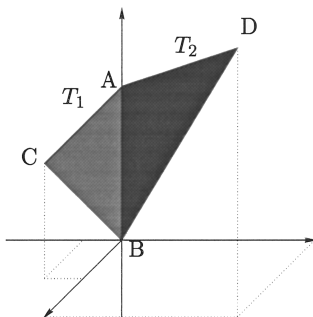


FIG. 3. Two triangle is 3-space sharing an edge.

We set  $k = -(1/2) \int f_{12}(X, Y)dX$  and  $h = (1/2) \int f_{12}(X, Y)dY$ . Thus,  $f_{12}(X, Y) = (\partial k / \partial X) - (\partial h / \partial Y)$ . Let us consider the right-hand side of Green's formula. The right-hand side can be computed over a polygonal chain by summing the contribution of each segment, let us consider without loss of generality the first edge. Switching to local parametric coordinate  $t$

$$X = (X_1 - X_0)t + X_0$$

$$Y = (Y_1 - Y_0)t + Y_0,$$

we can turn the right-hand side of (21) into an integral in  $t$  and integrating in the range  $[0, 1]$ . What is left after the integration in  $t$  is a polynomial in the quantities  $X_0, Y_0, X_1, Y_1$ .  $\square$

**6.2. COMBINATORIALLY INVARIANT REGIONS ON THE SPHERE.** The set  $Vert(u)$  depends on  $u$ . In this section, we show how to divide the sphere  $U$  into regions such that in each region  $Vert(u)$  is combinatorially invariant.

Let us consider two triangles in 3 space,  $T_1$  and  $T_2$ . If we change  $u$  continuously,  $Vert(u)$  changes from one combinatorial fingerprint to another when the projection of three vertices is collinear. Let us call a *transition curve* the locus of points in  $U$  for which three specified vertices are collinear. Every such locus is a great circle on  $U$ . The collection of such great circles form an arrangement on  $U$  and every 2-dimensional cell of such an arrangement corresponds to a set of directions for which  $Vert(u)$  is combinatorially invariant. Thus, one such region  $R_j$  is bounded by arcs of great circles and is a "convex" polygon in spherical geometry.

*Remark 1.* Note that the number of regions depends only on the six vertices of the two triangles and it is thus a constant. This is the only place in the paper where working with triangles is different from working with, say, quadrilaterals.

In order to give a more concrete feeling of the regions, we discuss the case of two triangles sharing an edge in the next subsection.

**6.2.1. Triangles Sharing an Edge.** Now let us consider as an example two specific triangles sharing an edge. Let us take the triangles  $T_1 = (A, B, C)$  and  $T_2 = (A, B, D)$ , sharing edge  $AB$ , which we place on the  $z$ -axis, as shown in Figure 3.

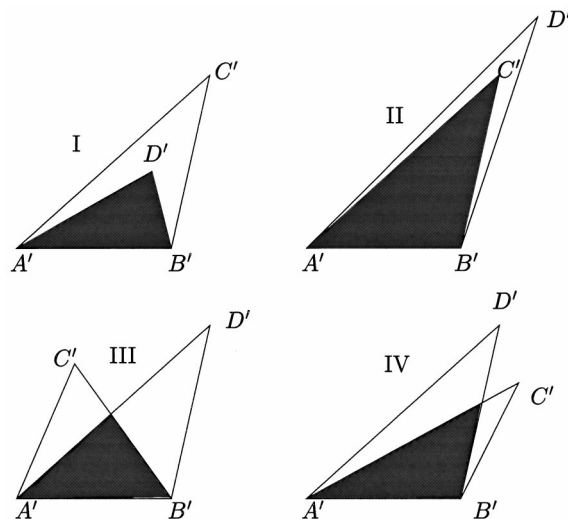


FIG. 4. Four different combinatorial types of projections.

We denote with the square brackets the determinant of three points in the local coordinates of the plane on which they lay, in the given order, with the last column filled with 1. The sign of this determinant denotes the relative orientation of the three points. For a generic point  $p \in R^3$  we denote with  $p'$  the point in local coordinates  $(X, Y)$  obtained by projecting  $p$  onto  $P(u)$ . Note that the projection of a triangle is still a triangle even in local coordinates and it is completely determined by the projections of the vertices.

Let us consider  $T'_1 = A'B'C'$ , and the lines defined by pairs  $(A'B')$ ,  $(A'C')$  and  $(B'C')$ . Suppose moreover that  $[A'B'C'] > 0$ . The formula to compute  $A_{12}(u)$  depends on the position of  $D'$  in the arrangement of the three lines defined above. Four combinatorially different projections with non zero area are shown in Figure 4. The corresponding regions (see Figure 5) on the sphere are:

*Region I.*  $D' \in T'_1$ . In this case, we have  $T'_2 \subset T'_1$  and  $Vert(u) = Vert(T'_2)$ . In order to have this case, the following conditions must be satisfied:

$$\begin{aligned} [A'B'D'] &> 0 \\ [B'C'D'] &> 0 \\ [C'A'D'] &> 0. \end{aligned}$$

*Region II.* Here  $T'_1 \subset T'_2$ ; thus,  $Vert(u) = Vert(T'_1)$ . This formula is used under the following conditions:

$$\begin{aligned} [A'B'D'] &> 0 \\ [B'C'D'] &< 0 \\ [C'A'D'] &< 0. \end{aligned}$$

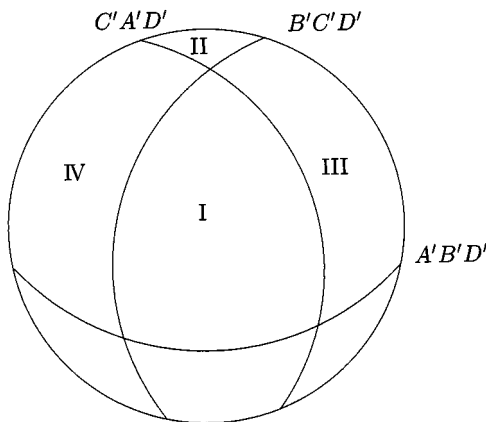


FIG. 5. Four relevant regions on the sphere.

*Region III.* Here the edge  $A'D'$  meets edge  $B'C'$ . The conditions for this case are:

$$[A'B'D'] > 0$$

$$[B'C'D'] < 0$$

$$[C'A'D'] > 0.$$

The area  $Vert(u) = \{A', B', (A'D' \cap B'C')\}$ . Note that one point of  $Vert(u)$  is not defined when  $D'A'$  is parallel to  $B'C'$ .

*Region IV.* Here  $B'D'$  meets edge  $A'C'$ . The conditions are:

$$[A'B'D'] > 0$$

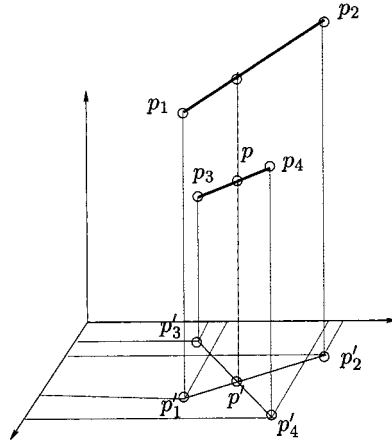
$$[B'C'D'] > 0$$

$$[C'A'D'] < 0.$$

We have  $Vert(u) = \{A', B', (A'C' \cap B'D')\}$ . Note that one point of  $Vert(u)$  is not defined when  $B'D'$  is parallel to  $A'C'$ .

**6.3. THE FORBIDDEN CURVE AND THE FORBIDDEN VECTOR.** Points in  $Vert(u)$  are of two types. They are either projections of vertices of the input triangles, or they are intersections of the lines spanning projections of edges of input triangles. Points of the first type are defined for any value of  $u$ . Points of the second type might not be defined for some direction  $u$ . We prove the following lemma:

**LEMMA 7.** *Let  $p' \in Vert(u)$  be the intersection of the lines defined by pairs of points  $(p'_1 p'_2)$  and  $(p'_3 p'_4)$ . Then  $p'$  is the projection of a point  $p \in R^3$  whose*

FIG. 6. Intersection point  $p'$  as projection of point  $p$ .

coordinates are of the form:

$$p_x = \frac{h_x}{w \cdot u} + k_x$$

$$p_y = \frac{h_y}{w \cdot u} + k_y$$

$$p_z = \frac{h_z}{w \cdot u} + k_z,$$

where  $w$ ,  $h_x$ ,  $h_y$ ,  $h_z$ ,  $k_x$ ,  $k_y$  and  $k_z$  are polynomials in the coordinates of  $p_1$ ,  $p_2$ ,  $p_3$  and  $p_4$ .

PROOF. Consider (as in Figure 6) the two skew lines  $p_1p_2$  and  $p_3p_4$ . They define a unique family of parallel planes that are parallel to both. Let  $w$  be the normal vector of such a family. The set of directions  $u$  for which the two lines  $p_1p_2$ ,  $p_3p_4$  project onto parallel lines in given by  $w \cdot u = 0$ , which is a linear combination of the quantities  $u_x$ ,  $u_y$ ,  $u_z$ .

Now we derive the expression for the intersection of  $p'_1p'_2$  and  $p'_3p'_4$ . Consider a point  $p(l)$  on the line  $p_3p_4$ , consider the plane through  $p_1$ ,  $p_2$  and  $p_1 + u$ . We want to find the point  $p(l)$  that belongs to that plane. Such a point, when projected in direction  $u$  is the intersection of the lines  $p'_1p'_2$  and  $p'_3p'_4$ . Thus, it is sufficient to equate the 4-by-4-determinant of the four points to zero, that is,

$$[p_1, p_2, p_1 + u, p(l)] = 0.$$

Since each coordinate of the variable point is of the form:  $p_x(l) = (x(p_3) - l)/(x(p_3) - x(p_4))$  (or  $p_x(l) = x(p_3)$ , if  $x(p_3) = x(p_4)$ ), developing the determinant by the last row we obtain a linear equation in  $l$ . The coefficient of  $l$  is a linear combination, whose coefficients depend on  $p_1$ ,  $p_2$ ,  $p_3$ ,  $p_4$ , of minors of the matrix  $[p_1, p_2, p_1 + u]$ , developing each minor on the last row we obtain a linear combination of  $(u_x, u_y, u_z)$ . Going back, we have that  $l =$



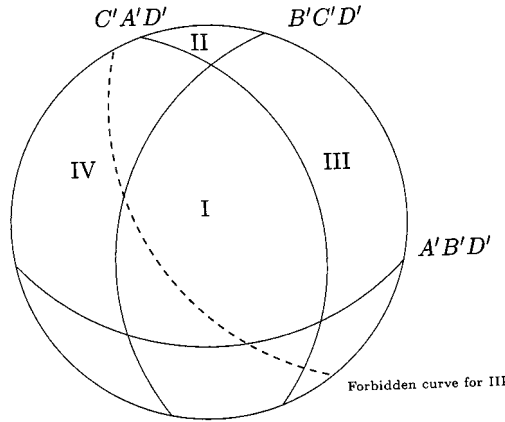


FIG. 7. Forbidden curve of region III.

$g(p_1, p_2, p_3, p_4)/LC(u_x, u_y, u_z)$ ; therefore, also the coordinates of the point  $p(l)$  have the same form. The projection has no influence on the denominator. So we have proved that the denominator of the expressions for the intersection point in local coordinate is a rational polynomial whose denominator contains a linear combination of the components of  $u$ . This term must then be  $w \cdot u$ , since this must be a factor, but it is the only factor.  $\square$

We will call  $w$  the *forbidden vector* for  $p'$  and the great circle  $w \cdot u = 0$  the *forbidden curve* of  $p'$  (see Figure 7). Next, we state a few useful properties of regions.

LEMMA 8. *The closure of a region  $R_j$  does not intersect forbidden curves from vertices of its fingerprint set  $Vert_j$ .*

PROOF. It follows from the fact that within the validity region the formula represents the integral of a bounded function over a bounded domain such a value does not diverge; therefore, there can be no point in common between a regions and forbidden curves.  $\square$

We state without proof the next lemma.

LEMMA 9. *The intersection for a region and a great circle is a connected arc of great circle.*

6.4. THE SUBDOMAINS. By a spherical polygon, we mean a compact subset of the sphere whose boundary is the union of arcs of great circles.

From the discussion in the first part of this section, we have that the triangles  $T_1$  and  $T_2$  in  $R^3$  induce on the sphere of directions an arrangement of great circles  $\mathcal{A}$ . Each cell  $R_j$  of such an arrangement is a spherical polygon with the property that the representation of the area function  $A_{12}$  is combinatorially invariant. Next we show how to split each such cell  $R_j$  into either quadrangular or triangular spherical polygons. Moreover we distinguish the great circle, that is the locus of point  $u$  on the sphere such that  $\cos \phi = 0$ . Let us call  $W$  such great circle. A few definitions:

Let  $e$  be an arc of great circle, we call  $GC(e)$  the great circle spanning  $e$ . Let  $u_1$  and  $u_2$  be distinct points on the unit sphere, we call  $SCG(u_1, u_2)$  the unique

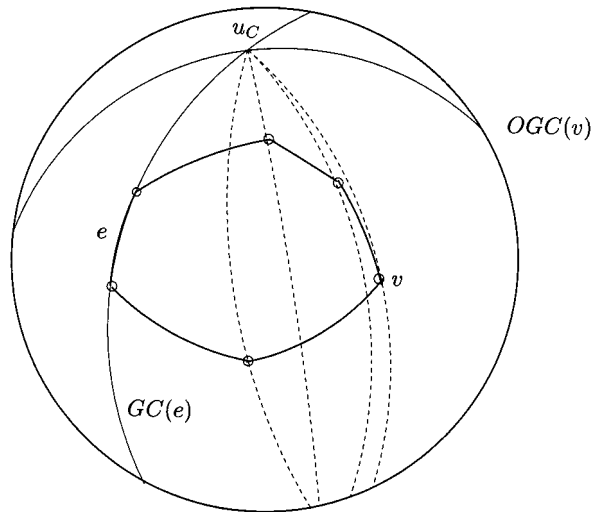


FIG. 8. Slicing of a spherical polygon into sub-regions.

great circle incident to them. Let  $u_1$  be a point on the unit sphere, by  $OCG(u_1)$  we denote the locus of directions orthogonal to  $u_1$ , which is a great circle.

Next we show how to subdivide each region  $R_j$  into subdomains.

*Case (1).*  $R_j$  does not have  $W$  on its boundary. In this case, we can choose any edge  $e$  and a vertex  $v$  not adjacent to  $e$ . Let us call  $u_C$  the intersection of the great circle  $GC(e)$  and  $OGC(v)$ . Take  $u_C$  as the “cutting pole” for  $R_j$  by drawing all great circles  $SCG$  through  $u_C$  and the vertices of  $R_j$ . This set of great circles slices  $R_j$  into a possibly empty set of spherical quadrilaterals and one spherical triangle incident on  $v$ . Note that in our construction the angle between  $v$  and  $u_C$  is  $\pi/2$ .

*Case (2).*  $R_j$  has one edge that belongs to  $W$ . Let us call such an edge  $e_W$ . In this case, we must choose  $e = e_W$  and perform the previous operations at case (1). Note that the only subdomain where  $\cos \phi = 0$  is the one adjacent to  $e_W$ .

To summarize we have four types of subdomains: quadrangular and not adjacent to  $W$ , triangular and not adjacent to  $W$ , quadrangular and adjacent to  $W$ , and triangular and adjacent to  $W$ . An example is shown in Figure 8.

## 6.5. LOCAL COORDINATE SYSTEM ON THE UNIT SPHERE

**6.5.1. Quadrangular Subdomains.** Here we assume that the sub-domain  $D = R_j$  is quadrangular, with edges  $e_1, e_2, e_3, e_4$ , where  $e_1$  and  $e_3$  are the result of the slicing and  $e_2, e_4$  are portions of edges of  $D$ . Consider the intersection point  $u_D$  among the great circles  $CG(e_2)$  and  $GC(e_4)$ . In this case the joining great circle of  $u_C$  and  $u_D$ ,  $GC(u_C, u_D)$ , does not intersect the boundary of  $D$  since  $D$  is the intersection of a spherical wedge based on  $u_C$  and a spherical wedge based on  $u_D$ . A spherical wedge can be defined by a planar angle at the pole of the wedge. Let us consider the points  $u_C, u_D$  and the point  $u_{CD}$  that is orthogonal to both. They form a skewed triple of versors. Call  $u_{CDD}$  the point orthogonal to  $u_{CD}$  and  $u_D$ . Call  $u_{CDC}$  the point orthogonal to  $u_{CD}$  and  $u_C$ . We have two orthogonal reference frames  $B = (u_{CD}, u_{CDC}, u_C)$  and  $S = (u_{CD}, u_{CDD}, u_D)$ . We intro-

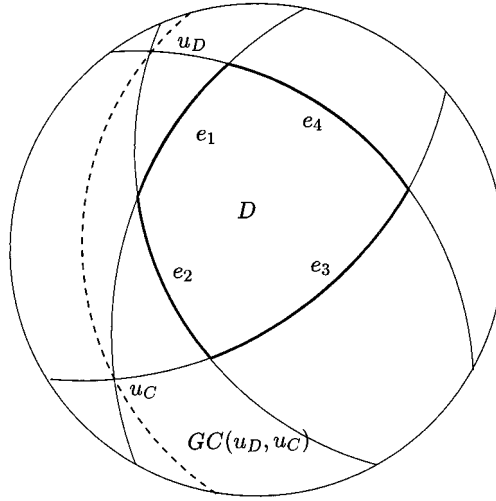


FIG. 9. Determination of points  $u_C$  and  $u_D$  for a spherical quadrilateral.

duce local versors and coordinate notation: Let  $B$  be a reference frame ( $i_B$ ,  $j_B$ ,  $k_B$ ) where  $i_B$  points up,  $k_B$  to the left, and  $j_B$  towards the viewer (see Figures 9 and 10).

Projecting from  $j_B$  we see on the projection plane the  $x_B$  and  $z_B$  axis, let us call  $\alpha_B$  the angle that the projection of  $u$  forms with the (vertical)  $x_B$ -axis, and  $a_B$  is tangent so:

$$a_B = \tan \alpha_B = \frac{u_{Bz}}{u_{Bx}}.$$

Projecting from  $k_B$  we see the  $x_B$  and  $y_B$  axis, let us call  $\beta_B$  the angle that the projection of  $u$  makes with the  $x_B$  axis, and  $b_B$  its tangent so:

$$b_B = \tan \beta_B = \frac{u_{yB}}{u_{Bx}}.$$

Calling

$$H = \sqrt{1 + a_B^2 + b_B^2},$$

we have:

$$u_{xB} := \frac{1}{H},$$

$$u_{yB} := \frac{b_B}{H},$$

$$u_{zB} := \frac{a_B}{H}.$$

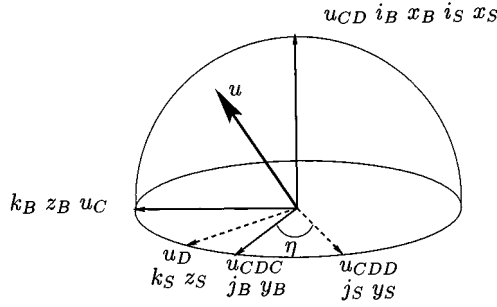


FIG. 10. Construction of Base reference and Slanted reference frames.

Now, we consider the slanted reference frame  $S$ . Let  $S$  be a reference frame  $(i_S, j_S, k_S)$ . The  $x_S$ -axis points at the middle of the hemisphere. We obtain  $S$  by rotating  $B$  of an angle  $\eta$  using the  $x_B$  axis as axis of rotation. Therefore,  $i_B = i_S$ . In matricial form:

$$\begin{pmatrix} i_S \\ j_S \\ k_S \end{pmatrix} = \begin{pmatrix} 1 & 0 & 0 \\ 0 & \cos \eta & \sin \eta \\ 0 & -\sin \eta & \cos \eta \end{pmatrix} \begin{pmatrix} i_B \\ j_B \\ k_B \end{pmatrix}. \quad (22)$$

Inverting the matrix:

$$\begin{pmatrix} u_{xS} \\ u_{yS} \\ u_{zS} \end{pmatrix} = \begin{pmatrix} 1 & 0 & 0 \\ 0 & \cos \eta & \sin \eta \\ 0 & -\sin \eta & \cos \eta \end{pmatrix} \begin{pmatrix} u_{xB} \\ u_{yB} \\ u_{zB} \end{pmatrix}. \quad (23)$$

We define the angles with respect to the  $S$ -reference frame.

Projecting from  $j_S$ , we see in the projection plane the  $x_S$  and  $z_S$  axis, let us call  $\alpha_S$  the angle that the projection of  $u$  forms with the (vertical)  $x_S$ -axis, and  $a_S$  is tangent so:

$$a_S = \tan \alpha_S = \frac{u_{zS}}{u_{xS}}.$$

Projecting from  $k_S$ , we see the  $x_S$  and  $y_S$  axis, let us call  $\beta_S$  the angle that the projection of  $u$  makes with the  $x_S$  axis, and  $b_S$  its tangent so:

$$b_S = \tan \beta_S = \frac{u_{yS}}{u_{xS}}.$$

Dividing both sides of this identity

$$u_{yS} = (\cos \eta)u_{yB} + (\sin \eta)u_{zB}$$

by  $u_{xS}$ , we obtain:

$$b_S = (\cos \eta)b_B + (\sin \eta)a_B,$$

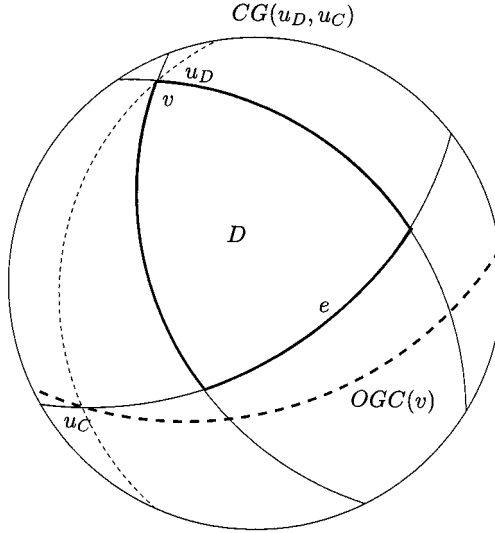


FIG. 11. Determination of points  $u_C$  and  $u_D$  for a spherical triangle.

and therefore:

$$a_B = \frac{1}{\sin \eta} (b_S - (\cos \eta) b_B).$$

We choose as our local coordinates system for the sub-domain  $D$  the pair of parameters  $(\alpha_j, \beta_j) = (b_B, b_S)$ . We use the above equality to re-express  $H$  and the components of  $u_B$  in  $B$  as a function of  $b_B$  and  $b_S$ .

*Triangular subdomains.* Here we assume that  $D$  is a triangular subdomain. Therefore, it is adjacent to  $v$  and, using the notation of the previous case  $u_D = v$ .  $D$  is the intersection of a spherical wedge based on  $u_C$  and a spherical wedge based on  $v$ . The great circle  $GC(u_C, v)$  meets the boundary of  $D$  in  $v$ . On the other hand by construction  $v$  and  $u_C$  are at an angle of  $\pi/2$ . Therefore reference frames  $B$  and  $S$  are obtained one from the other by a rotation of  $\pi/2$ . Consider angles  $\alpha_B$  and  $\beta_B$ . Let the range for  $\beta_B$  be  $[\beta_0, \pi/2]$  so that the range for  $b_B$  is  $[\tan \beta_0, +\infty]$ . We can always choose  $0 < \beta_0 < \pi/2$  (see Figures 11 and 12). We take an angle  $\gamma = \beta - \beta_0$  so that calling  $e = \tan \beta_0$  and  $c_B = \tan \gamma$  we have:

$$c_B = \frac{b_B + e}{1 - b_B e}.$$

The range of integration now is  $c_B \in [0 \cdots \tan(\pi/2 - \beta_0)]$  and  $c_B$  does not diverge in this interval (although  $b_B$  would). Inverting the relation:

$$b_B := \frac{c_B - e}{1 + e c_B}. \quad (24)$$

Now we choose as our local coordinates on the sphere  $(\alpha_j, \beta_j) = (a_B, c_B)$ . We can now express  $H$ , and the components of  $u_B$  as a function of  $a_B$  and  $c_B$ .

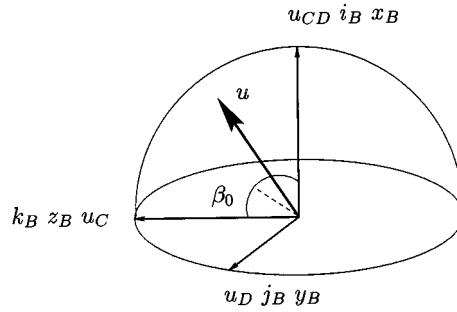


FIG. 12. Construction of Base reference frame and angle shift.

6.6. THE DIFFERENTIAL MEASURE OF DIRECTIONS IN LOCAL COORDINATES. From Santalo [1976], we take this form of the differential element of directions:

$$du = \frac{du_{zB} \wedge du_{yB}}{u_{xB}}. \quad (25)$$

*Quadrangular subdomains.* In order to express  $du$  in terms of  $b_B$  and  $b_S$  we need to compute the determinant of the Jacobian  $J$  of the functions  $u_{yB}$  and  $u_{zB}$  with respect to the parameters  $b_B$  and  $b_S$ . We obtain:

$$J = -\left(\frac{1}{\sin \eta}\right)\left(\frac{1}{H^4}\right).$$

Note that for  $\eta \neq 0$  this expression does not diverge for any real value of  $a_B$  and  $a_S$ . From (25), we have  $du = |JH|db_B \wedge db_S$ , thus

$$du = \left|\left(\frac{1}{\sin \eta}\right)\left(\frac{1}{H^3}\right)\right|db_B \wedge db_S.$$

*Triangular subdomains.* We express  $H$  and the components of  $u_B$  in the  $B$  reference system in terms of  $a_B$  and  $c_B$  by using (24). We obtain

$$H = \frac{M}{(1 + ec_B)},$$

where

$$M = \sqrt{(1 + ec_B)^2(1 + a_B^2) + (c_B - e)^2}. \quad (26)$$

The determinant  $J$  of the Jacobian of the functions  $u_{yB}$  and  $u_{zB}$  with respect to parameters  $a_B$  and  $c_B$  is:

$$J = \frac{-(1 + e^2)(1 + ec_B)^2}{M^4},$$

so

$$du = |JH|dc_B \wedge da_B = \frac{(1 + e^2)(1 + ec_B)}{M^3} dc_B \wedge da_B.$$

Notice that  $M$  is the square root of a sum of squares, and it cannot be zero for any real value of  $e$ ,  $c_B$  and  $a_B$ .

6.7. THE PROJECTION TRANSFORMATION. Lemma 6 states that the area function  $A_{12}(u)$  is a polynomial in the coordinates of the vertices  $Vert(u)$  in local coordinates. In order to complete our description, we need to give the transformation matrix that represents the projection operation in direction  $u$ . It is sufficient to give the matrix in the coordinates  $u_B$ . Denoting with the subscript  $P$  the local reference frame on  $P(u)$  having  $u$  as  $k_P$ -axis:

$$\begin{pmatrix} i_P \\ j_P \\ k_P \end{pmatrix} = \begin{pmatrix} \frac{u_{Bz}u_{Bx}}{G} & \frac{u_{By}u_{Bz}}{G} & -G \\ -u_{yB} & u_{xB} & 0 \\ G & G & u_{zB} \end{pmatrix} \begin{pmatrix} i_B \\ j_B \\ k_B \end{pmatrix}, \quad (27)$$

Where  $G = \sqrt{u_{xB}^2 + u_{yB}^2}$ . In terms of coordinates:

$$\begin{pmatrix} x_P \\ y_P \\ z_P \end{pmatrix} = \begin{pmatrix} \frac{u_{Bz}u_{Bx}}{G} & \frac{-u_{By}}{G} & u_{xB} \\ \frac{u_{yB}u_{Bz}}{G} & \frac{u_{xB}}{G} & u_{yB} \\ -G & 0 & u_{zB} \end{pmatrix} \begin{pmatrix} x_B \\ y_B \\ z_B \end{pmatrix}. \quad (28)$$

The local coordinates of the projection are given by  $x_P$  and  $y_P$ . Using previously derived equalities we can express the components of  $u_B$  in terms of the local spherical coordinates  $(\alpha_j, \beta_j)$  for subdomain  $D_j$ .

### 7. Proof of Lemma 4 for BEM Integrals

The functions and sub-domains described in Section 6 satisfy by construction Properties (1) and (2) of Definition 1. In order to prove that Properties (3) and (4) are also satisfied we need to consider several subcases.

7.1. SUBDOMAINS NOT INCIDENTS TO  $\mathcal{W}$ . Let  $R_j$  be a subdomain not incident to  $\mathcal{W}$ . In this case, the kernel of the integral is:

$$f_j(u) = \frac{A_{12}(u)}{u \cdot n_2}.$$

Thus, restrictions of  $f_j$  are analytic provided that restrictions of  $u \cdot n_2$  and  $A_{12}(u)$  are analytic and  $u \cdot n_2 \neq 0$ . These conditions are equivalent to requiring that:  $H \neq 0$ ,  $G \neq 0$ ,  $u \cdot n_2 \neq 0$  and  $u \cdot w_F \neq 0$  for any forbidden vector  $F$  associated with  $R_j$ . Moreover, the condition  $H \neq 0$  also ensures that restrictions

of the function  $g(u)$  associated with the differential measure of direction are analytic.

7.1.1. *Coordinates  $(b_B, b_S)$ .* Recalling the coordinates in Section 6.5 for quadrangular sub-domains we have that  $H \neq 0$ , corresponds to the equation:  $1 + a_B^2 + b_B^2 = 0$ . Equivalently:

$$1 + \left( \frac{1}{\sin \eta} (b_S - (\cos \eta) b_B) \right)^2 + b_B^2 = 0.$$

For a fixed value  $\bar{b}_B$  we obtain two conjugated imaginary poles in the complex  $b_S$ -plane. We obtain similarly conjugated imaginary poles when we fix the  $\bar{b}_S$ .

Condition  $G \neq 0$  corresponds to finding zeroes of  $b_B^2 + 1 = 0$ ; thus, for any fixed value  $\bar{b}_S$  we have poles at  $\pm i$  on the complex  $b_B$ -plane.

Note that the various transformations introduce only imaginary poles, not real ones. Let  $w$  be either a forbidden vector  $w_F$  or  $n_2$ . We show that the condition  $u \cdot w = 0$  introduces only real poles. Indeed  $u \cdot w = 0$  if and only if  $w_x + b_B w_y + (1/\sin \eta (b_S - (\cos \eta) b_B)) w_z = 0$ . Fixing either of the variables gives a linear equation in the other variable that has one real solution. Since in the range of the closed domain  $D_j$  the function  $f_j$  is bounded, then there is a rectangle  $Rect(\bar{b}_S)$  in the complex  $b_B$ -plane that strictly contains the real range  $I_{b_S}$  and none of the real or complex poles. Similarly, there is a rectangle  $Rect(\bar{b}_B)$  in the complex  $b_S$ -plane that strictly contains the real range  $I_{b_B}$  and none of the real or complex poles. This proves Properties (3) and (4) of Definition 1 for rectangular subdomains not incident to  $W$ .

7.1.2. *Coordinates  $(a_B, c_B)$ .* Recalling the coordinates in Section 6.5 for triangular sub-domains we have that  $H = 0$  if and only if  $M = 0$ . From formula (26), we see that for a fixed value  $\bar{c}_B$  we have either no roots or complex conjugated roots. For a fixed  $\bar{a}_B$  equation  $M = 0$  cannot have real roots in  $c_B$ . It is easy to see this by contradiction. If we suppose the existence of a real root we would have that the sum of two nonnegative numbers is null, which is possible only if both  $(1 + ec_B)$  and  $(c_B - e)$  are simultaneously zero. This is not possible for any real value of  $e$ . Thus, also in this case, we have two complex conjugated roots. Condition  $G = 0$  is rewritten as

$$1 + \left( \frac{c_B - e}{1 + ec_B} \right)^2 = 0.$$

Again, by contradiction it is easy to see that this equation cannot have real roots.

Let  $w$  be either a forbidden vector  $w_F$  or  $n_2$ . We show that the condition  $u \cdot w = 0$  introduced only real poles. Indeed  $u \cdot w = 0$  iff

$$(1 + ec_B)(w_x + a_B w_z) + (c_B - e)w_y = 0$$

Again this is a bilinear equation, therefore any restriction is a linear equation giving one real root. As observed before these real roots cannot be incident to the real closed domains  $I_{c_B}$  or  $I_{a_B}$ , therefore we have rectangles  $Rect(\bar{c}_B)$  and  $Rect(\bar{a}_B)$  as defined in Definition 1. This proves Properties (3) and (4) of Definition 1 for triangular subdomains not incident to  $W$ .



7.2. SUBDOMAINS INCIDENT TO  $W$ . In this subsection, we use generic coordinates  $(\alpha, \beta)$  to denote either  $(b_B, b_S)$  or  $(c_B, a_B)$ . Suppose without loss of generality that in the local coordinate system  $LCS_j$  associated with  $D_j$  we have  $\cos \phi = 0$  for  $\alpha = \alpha_0$ .

7.2.1. *Restrictions  $\beta = \bar{\beta}$ .* The proof of the previous subsections implies that our function  $f_j(u)g(u)$  is analytic in a punctured rectangle  $Rect(\bar{\beta}) \setminus \{\alpha_0, 0\}$  in the complex plane. From Theorem 1, we know that the real univariate function  $f_j(\alpha, \bar{\beta}) = K'(\alpha, \bar{\beta})$  admits at  $\alpha = \alpha_0$  the real extension  $K''(\alpha_0, \bar{\beta})$ .

At this point, we invoke a classical result in complex analysis (see e.g., Evgrafov [1996] and Conway [1973]), stating that an analytic extension along a path on the complex plane is independent of the chosen path. Therefore, the extension of  $f_j(\alpha, \bar{\beta})$  as a real function is also a complex extension. This shows that our univariate restrictions of  $f_j(u)g(u)$  admits a complex analytic extension within  $Rect(\bar{\beta})$ , thus satisfying Property (4) in Definition 1.

7.2.2. *Restrictions  $\alpha = \bar{\alpha}$ .* Proofs in the previous subsections show that for any  $\bar{\alpha} \neq \alpha_0$  the restriction  $f_j(\bar{\alpha}, \beta)g(\bar{\alpha}, \beta)$  admits a complex analytic extension in a certain rectangle on the complex plane. Thus to complete the proof it is sufficient to show that  $f_j(\alpha_0, \beta) = K''(\alpha_0, \beta)$  admits an analytic extension in a rectangle of the complex  $\beta$ -plane. We refer to the initial treatment in Section 3.3 and to the integral geometric formula (19) for  $K''(u)$ .

The general flavor of this section is to follow the blueprint of the discussion in Sections 6 but on a 1-dimensional domain (the great circle  $W$ ) instead of a two dimensional one (the sphere of directions).

Let us consider triangles  $T_1 = (p_1, p_2, p_3)$  and  $T_2 = (p_4, p_5, p_6)$  in the reference frame  $J = (n_2, n_2 \times u, u)$  associated with the plane  $P(u)$ . Moreover, we consider the distinguished points  $p_7, p_8$ , and  $p_9$  which are the intersections of the lines spanning the edges of  $T_1$  with the plane spanning  $T_2$ .

Note that the mapping between the  $B$ -reference frame and the  $J$ -reference frame is polynomial in the components of  $u_B$  since normalization is not needed. Since  $u \cdot n_2 = 0$ , the projection  $T'_2$  of  $T_2$  in direction  $u$  is a degenerate triangle (i.e., a segment). Using the notation in Section 3.3, we have that  $z_J = z$  and  $y_J = \eta$ .

The great circle  $W$  on the unit sphere is subdivided into arcs of great circles such that in each such arc the intersection  $T'_{12} = T'_1 \cap T'_2$  is combinatorially invariant, that is the relevant features of  $T'_{12}$  are defined by a combinatorially invariant set of features (vertices and edges) of the input triangles. It is easy to see that the combinatorial fingerprint of  $T'_{12}$  changes for directions in which 3 vertices or distinguished points of the input triangles are collinear, therefore the subdivision of  $W$  is just the trace on  $W$  of the transition curves defined in Section 6.2 for the whole sphere. Therefore, each such arcs coincide with sides of subdomains as defined in Section 6.4.

The relevant features of  $T'_{12}$  are its end points that may be the projection of an endpoint of  $T_2$  or the projection a distinguished point. It is also possible that the projection of a vertex of  $T_2$  is interior to  $T'_{12}$ . In this case  $T'_{12}$  is the concatenation of two combinatorial segments. We will show that, in each such arc of  $W$ , integrals (18) and (19) are defined by functions that have Property (3) of Definition 1. We use the following lemma:

LEMMA 10. *Integral  $M_\eta$  defined in (18) is expressible as a rational function in the local coordinates of endpoints of the triangles and distinguished points and a polynomial in the variable  $\eta$ .*

PROOF. Let  $\sigma_2(x_B, y_B, z_B(x_B, y_B))$  be the density function associated with the second triangle. Considering the transformation in local J-coordinate, we have  $\sigma_2(p_J) = \sigma_2(x(p_J), y(p_J), z(x(p_J), y(p_J)))$ . Since  $\sigma_2$  is supposed polynomial in the coordinates  $(x_B, y_B, z_B)$  it is also polynomial in the components of  $p_J$  and the entries of the transformation matrix, which as observed before are polynomials in the components of  $u_B$ . Since for choice of coordinates  $x_J = 0$  in the domain of interest, we have that  $\sigma_2 = \sigma_2(x_J, z_J) = \sigma_2(\eta, z)$  is a polynomial in the coordinates  $\eta$  and  $z$  and in the components of  $u_B$ . Thus, the antiderivative in  $z$  has the same properties. The extremes of the integral (18) can be expressed by interpolation of the end-points of the relevant segments expressed as a linear functions of  $\eta$  whose coefficients are rational functions in the local coordinates of the end-points of the segment.  $T'_{12}$ .  $\square$

Repeating the above argument for  $\sigma_1(p_B)$  we can conclude that the kernel in integral (19) is polynomial in  $\eta$  and so is its antiderivative. The limit of integration of (19) are expressed by the endpoints of  $T'_{12}$  in local coordinates. To summarize,  $K''(u)$  is expressible as a sum of rational functions of the vertices and of the input triangles and distinguished points in local  $J$ -coordinates. The directions for which the denominator of the resulting rational function is zero (forbidden directions) are directions corresponding to the edges of  $T_2$ . However,  $K''(u)$  is bounded for any value of  $u \in W$ ; therefore, we obtain real analytic extension by substituting the limit of the function in those directions for which the denominator of the rational function is zero.

To conclude, the mapping from the  $(\alpha_0, \beta)$ -coordinates to the components of  $u_B$  introduces only imaginary poles, while the mapping from the components of  $u_B$  to  $K''(u)$  does not introduce any real pole. Therefore,  $K''(\beta)$  admits an analytic extension in a rectangle of the complex plane that includes properly the interval  $I_\beta$ . This concludes the proof of Lemma 4.

## 8. Proof of Lemma 5 for Volume-to-Volume Integrals

Consider two convex polyhedra  $B_1$  and  $B_2$  endowed with volume charge density  $\rho_1$  and  $\rho_2$ . Let  $B'_{12}(u)$  be the intersection of the projections of  $B_1$  and  $B_2$  onto the plane  $P(u)$  of normal  $u$ . Let  $M_{12}(u)$  be the planar map induced by the projections onto  $P(u)$  of the edges of  $B_1$  and  $B_2$ . The planar map  $M_{12}(u)$  is composed of open faces that are either disjoint from  $B'_{12}$  or completely contained in it (we will call these faces *internal*). Each inner face is completely contained in the projection of two facets of  $B_1$  and two facets of  $B_2$  which we call the *covering facets*.

We prove the following lemma, which is analogous to Lemma 6.

LEMMA 11. *The integral  $V_{12}(u)$  defined by formula (6) is expressible as a rational function in the coordinates of the vertices of the inner faces of  $M_{12}(u)$  and of the vertices of the corresponding covering facets in local coordinates.*

PROOF. Let us call  $(X, Y, Z)$  the local coordinate system. The transformation from absolute coordinates to the local coordinates is linear in the local coordi-

nates and the entries of the transformation matrix. Thus  $\rho_1(X, Y, Z)$  is a polynomial in  $X, Y, Z$ . Let us consider the inner face  $f$  and let  $Z = Z_1(X, Y)$ , and  $Z = Z_2(X, Y)$  be the equations of the planes spanning the two covering faces of  $B_1$ . Such two functions  $Z_1$  and  $Z_2$  are linear functions in  $X$  and  $Y$ , whose coefficients are rational functions of the coordinates of 3 vertices of the covering facets. This can be seen easily by writing the equation of the plane in the form of a determinant. The weight of a line parallel to  $u$  passing through the point  $(X, Y) \in f$ , relative to the first body is:

$$m_1(X, Y) = \int_{Z_1(X, Y)}^{Z_2(X, Y)} \rho_1(X, Y, Z) dZ.$$

Thus,  $m_1(X, Y)$  is a polynomial in  $X$  and  $Y$  whose coefficients are rational functions of the coordinates of vertices of the covering facets. A similar property holds for  $m_2(X, Y)$ , the weight relative to the second body. Finally, using Green's formula as in Lemma 6, we can express  $\int_{(X, Y) \in f} m_1 m_2 dX dY$  as a polynomial in the vertices of the face  $f$ .  $\square$

We subdivide the unit sphere into regions such that in each region the combinatorial fingerprint of the faces of  $M_{12}(u)$  (including the covering facets) is constant. Again, it is easy to show that each such region is a spherical convex polygon on the unit sphere and we can proceed as in Section 6. The situation is rather simplified since we do not have the  $W$  great circle. On the other hand, besides the forbidden vectors introduced by vertices of inner faces resulting from intersection of skew spatial edges, we have as forbidden vectors also the normals to the covering facets. Since  $V_{12}(u)$  does not diverge it is easy to conclude that also the new forbidden curves do not intersect the corresponding closed region on the unit sphere. We use the same coordinates and calculations as in Sections 6.4, 6.5, 6.6 and 6.7. Then an argument following the one in Section 7.1 is used to conclude the proof of Lemma 5.

## 9. Experimental Results

The Gaussian adaptive algorithm to compute the normal component of integral (2) using formula (14) has been implemented in *C* on a Pentium 100 processor running the Linux operating system and in Mathematica (version 2.2.2) under Windows '95. A more detailed description of the experiments is in Bientinesi and Pellegrini [1997].

*Input.* We made two sets of experiments with triangles sharing an edge. In the first experiment we set  $T_1 = \{(0, 0, -1), (0, 0, 1), (0, -1, 0)\}$  and  $T_2 = \{(0, 0, -1), (0, 0, 1), (\sin A, -\cos A, 0)\}$ , where the angle  $A$  assumes values  $\frac{3}{4}\pi, \pi/2, \pi/4, \pi/8, \pi/16, \pi/32$ . In the second experiment we set  $T_1 = \{(0, 0, -1), (0, 0, 1), (0, -1, -1)\}$  and  $T_2 = \{(0, 0, -1), (0, 0, 1), (-\sin B, 0, \cos B)\}$ , where the angle  $B$  assumes values  $\frac{1}{6}\pi$  for  $i = 1 \dots 5$ .

The first experiment is intended to study the dependency of the algorithm on the dihedral angle between the input triangles. The second experiment is intended to study the dependency on the aspect ratio of one of the two triangles. We set the surface density functions  $\sigma_1$  and  $\sigma_2$  to be constant and equal to 1.

TABLE I. NUMBER OF DIRECTIONS/RELATIVE ERROR.

Directions	$A = \pi/32$	$A = \pi/16$	$A = \pi/8$	$A = \pi/4$	$A = \pi/2$	$A = 3/4\pi$
24	(1)124	(2)793	(2)161	(2)224	(2)228	(2)189
54	(2)482	(2)191	(5)642	(3)377	(3)208	(3)151
96	(2)174	(3)401	(4)564	(4)515	(4)154	(5)961
216	(3)217	(4)111	(5)553	(6)978	(7)102	(7)417
486	(5)845	(6)468	(7)803	(9)269	(10)601	(10)126
1014	(8)299	(8)122	(9)258	(12)166	(13)15	(14)1
1536	-	(9)587	(11)671	(12)995	(13)12	-

TABLE II. SECONDS/RELATIVE ERROR.

Seconds	$A = \pi/32$	$A = \pi/16$	$A = \pi/8$	$A = \pi/4$	$A = \pi/2$	$A = 3/4\pi$
0.01	(1)124	(2)793	(2)161	(2)224	(2)228	(2)189
0.02	(2)482	(2)191	(5)642	(3)377	(3)208	(3)151
0.05	(2)174	(3)401	(4)564	(4)515	(4)154	(5)961
0.1	(3)217	(4)111	(5)553	(6)978	(6)102	(7)417
0.2	(5)845	(6)468	(6)336	(7)189	(10)601	(10)126
0.5	(7)299	(8)447	(9)258	(12)166	(13)11	(14)1
0.9	(8)157	(10)321	(11)342	-	-	-

*Reference Value.* Since we could not find analytic solutions to integral (2) or (14), we compute the reference value as follows. Starting with formulation (14) we compute the regions of the unit sphere as described in Section 6.2.1 and we express the area function (20) explicitly in spherical coordinates for each region. Using Mathematica, we integrate analytically in one of the variables and numerically on the second variable. The value returned by Mathematica is considered reliable up to 14 digits.

*Results.* We show the relative error using the notation  $(n_1)n_2$  where  $n_1$  is the number of zeroes after the decimal point, and  $n_2$  the significant digits. In Table I, we have the relative error for several values of the angle  $A$  as a function of the number of directions used in the numerical integration. In Table II, we give the relative error for experiment  $A$  as a function of time. Tables III and IV give the same information for experiment  $B$ . We give plots of relative error versus number of directions in logarithmic-logarithmic scale for experiment  $A = \pi/32$  (Figure 13),  $A = 4\pi/3$  (Figure 14),  $B = \pi/2$  (Figure 15) and  $B = 5\pi/6$  (Figure 16).

*Comments.* In experiment A, the Gauss adaptive algorithm attains errors between  $10^{-8}$  and  $10^{-14}$  for 1000 directions, moreover it produces a rather smooth plot in the range  $[10, 1000]$ , afterwards it suffer from numerical instabilities probably due to round-off. The lower end of the error range is attained for small dihedral angles ( $A = \pi/32$ ), while the high end is attained for angles close to  $\pi/2$ .

Experiment B shows errors in the range between  $10^{-8}$  and  $10^{-11}$  for the angles  $B$  between  $\pi/6$  and  $5\pi/6$ , after 1000 directions. Dependency of the error on the angles  $A$  and  $B$  is weak in the middle of the range, with slightly worse performance towards the extremes of the angle range. The computing time needed to attain the best precision in each experiment is in the range 0.5 to 1 second. These times should be considered indicative only since at the moment little effort has been put in optimizing the codes. Experimental evidence is

TABLE III. NUMBER OF DIRECTIONS/RELATIVE ERROR.

Directions	$B = \pi/6$	$B = 2/6\pi$	$B = 3/6\pi$	$B = 4/6\pi$	$B = 5/6\pi$
24	(3)735	(2)308	(2)643	(2)941	(1)109
54	(4)295	(3)480	(3)546	(2)118	(2)192
96	(3)129	(4)334	(4)999	(3)235	(3)52
216	(5)192	(5)101	(5)242	(5)925	(4)387
486	(7)473	(8)282	(7)108	(7)792	(6)802
1014	(10)212	(12)44	(11)86	(9)149	(8)486

TABLE IV. SECONDS/RELATIVE ERROR.

Seconds	$B = \pi/6$	$B = 2/6\pi$	$B = 3/6\pi$	$B = 4/6\pi$	$B = 5/6\pi$
0.01	(3)735	(2)308	-	(2)941	(1)109
0.02	(4)295	(3)48	(2)643	(2)118	(2)192
0.05	(3)129	(4)334	(4)999	(3)235	(3)52
0.1	(5)192	(5)101	(5)242	(5)925	(4)387
0.2	(7)473	(8)282	(7)108	(7)792	(6)802
0.5	-	(11)616	(11)144	(10)378	(8)194

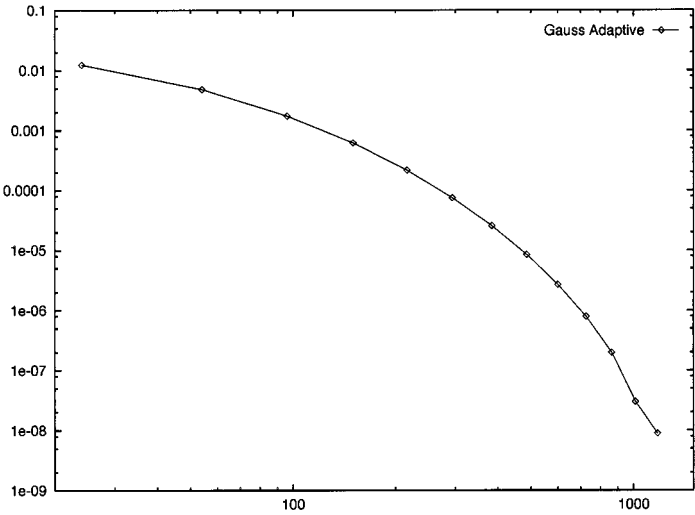


FIG. 13.  $A = \frac{\pi}{32}$ ; Directions/relative error.

consistent with the exponential error bound predicted in Section 5 for the Gauss adaptive method.

At the moment, we could not find in literature other comparable experimental data. Available data on alternative methods for computing surface-to-surface integrals [Hackbusch and Sauter 1993; Sauter and Schwab 1997; Erichsen and Sauter 1996] is relative to the solution of the linearized system with respect to an initial integral equation. This approach has the advantage that an analytic solution to the integral equation is found in the examples considered in Hackbusch and Sauter [1993], Sauter and Schwab [1997], and Erichsen and Sauter [1996], and is used as reference value. On the other hand, the outcome of the experiment is influenced by the choice of meshing strategy, by the choice of the functional basis and truncation of the functional expansion. Finally, if an

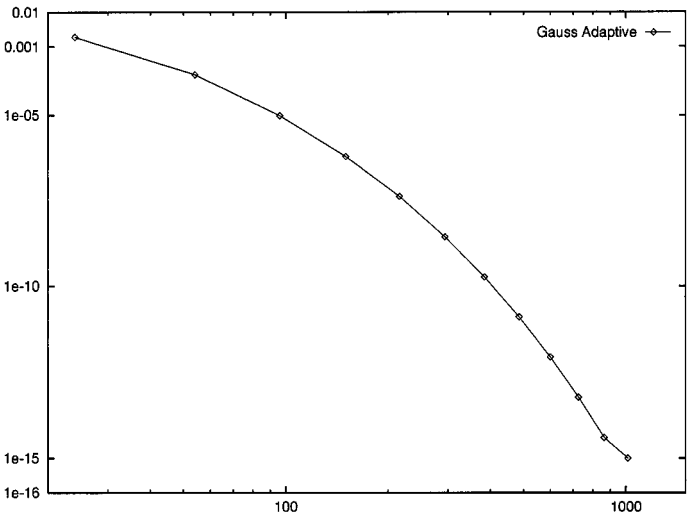


FIG. 14.  $A = \frac{4}{3}\pi$ ; Directions/relative error.

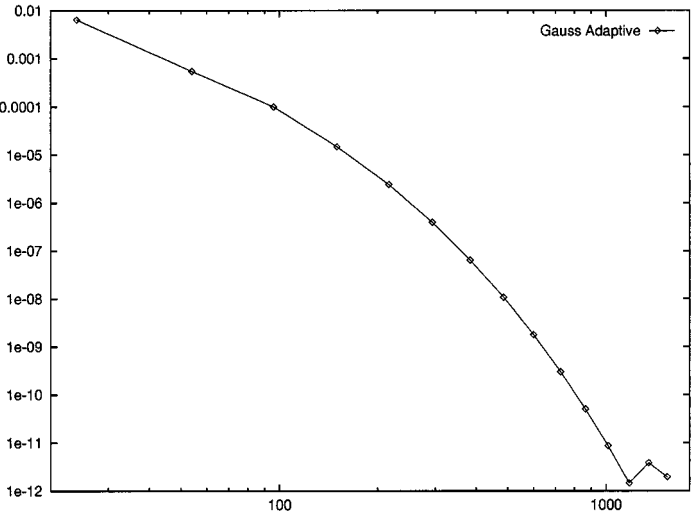


FIG. 15.  $B = \frac{3}{6}\pi$ ; Directions/relative error.

iterative method is used to solve the linear system, also the convergence of the iterative method influences the result. The computation of the entries of the stiffness matrix is just one of many critical steps. For the above reasons, although the preliminary experimental results are encouraging, further research is needed to integrate the proposed method of computing BEM integrals within a larger system.

10. Conclusions

In this paper, we give an integral geometric interpretation of the electrostatic forces between charged bodies and charged surfaces in 3-space. The main benefit of this interpretation is that the kernel of the resulting integral does not diverge.

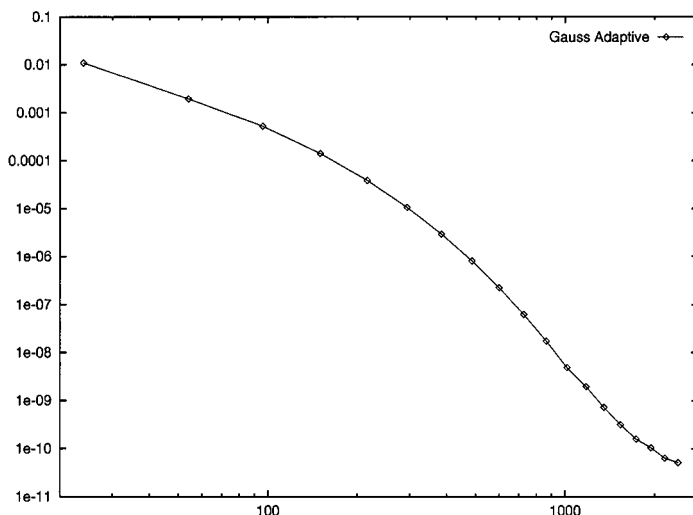


FIG. 16.  $B = \frac{5}{6}\pi$ ; Directions/relative error.

Based on such representation, we develop approximation algorithms with exponential error, which have better asymptotic bounds than previously known algorithms. Preliminary experimental data support the results of the theoretical analysis.

In the study of electrostatic fields, usually powerful differential and integral methods are used, however, at the best of my knowledge, a combination of methods from integral geometry, computational geometry and numerical analysis have not been significantly used so far to derive algorithms approximating electrostatic forces. We consider the novelty of the approach as important as the specific results obtained in this paper.

ACKNOWLEDGMENTS. I wish to thank Lawrence Coswar and Ken Clarkson for their observations on an early version. Two anonymous referees helped a lot with their comments and pointers at the relevant literature in numerical analysis and applied mathematics. Paolo Bientinesi has produced the experimental data, tables and plots.

#### REFERENCES

- APPEL, A. W. 1985. An efficient program for many-body simulations. *SIAM J. Sci. Statist. Comput.* 6, 85–103.
- BARNES, J., AND HUT, P. 1986. A hierarchical  $O(n \log n)$  force-calculation algorithm. *Nature* 324, 446–449.
- BIENTINESI, P., AND PELLEGRINI, M. 1997. Electrostatic fields without singularities: Implementations and experiments. Tech. Rep. IMC B4-97-16. Istituto di matematica computazionale del CNR, Via Santa Maria 46, Pisa, Italy. (Also [www.imc.pi.cnr.it/marcop/papiri/paolo-report.ps](http://www.imc.pi.cnr.it/marcop/papiri/paolo-report.ps).)
- BINNS, K. J., AND LAWRENSON, P. M. 1973. Analysis and computation of electric and magnetic field problems. Pergamon Press, Oxford, England.
- CADE, R. 1995. On discontinuous solutions of the integral equations of electrostatics. *IMA J. Appl. Math.* 55, 205–220.
- CALLAHAN, P. B., AND KOSARAJU, S. R. 1995. A decomposition of multidimensional point sets with applications to  $k$ -nearest-neighbors and  $n$ -body potential fields. *J. ACM* 42, 1 (Jan.), 67–90.
- CHIARI, M. V. K., AND SILVESTER, P. P., EDS. 1980. *Finite Elements in Electrical and Magnetic Field Problems*. Wiley, New York.



- CONWAY, J. B. 1973. *Functions of One Complex Variable*. Springer-Verlag, New York.
- COOLS, R. 1997. The approximation of low-dimensional integrals: Available tools and trends. In *Numerical Mathematics: Proceedings of the 15th IMACS World Congress on Scientific Computation, Modelling and Applied Mathematics*, A. Sydow, ed. (Berlin, Germany, Aug.). Vol. 2. Wissenschaft & Technik Verlag, pp. 469–474. (Also [www.cs.kuleuven.ac.be/publicaties/rapporten/tw/TW259.ps.gz](http://www.cs.kuleuven.ac.be/publicaties/rapporten/tw/TW259.ps.gz).)
- DAVIS, P. J., AND RABINOWITZ, P. 1975. *Methods of Numerical Integration*. Academic Press, Orlando, Fla.
- DUFFY, M. G. 1982. Quadrature over a pyramid or cube of integrands with a singularity at a vertex. *SIAM J. Numer. Anal.* 19, 6, 1260–1262.
- ERICHSEN, A., AND SAUTER, S. A. 1996. Efficient automatic quadrature in 3-D Galerkin BEM. Tech. Rep. TR-96-15. Berichtreihe des Mathematischen Seminars Christian-Albrechts-Universität zu Kiel Ludewig-Meyn-Str. D-24098, Kiel, Germany.
- ESPELID, T. O., AND GENZ, A., EDS. 1992. Numerical integration: Recent developments, software and applications. NATO ASI Series, vol. 357. Kluwer Academic Publishers, London, England.
- EVGRAFOV, M. A. 1966. *Analytical Functions*. Dover, New York.
- FINOCCHIARO, D. 1996. Monte Carlo evaluation of electrostatic potential and potential energy. Tech. Rep. TR-IMC B4-96-12. Istituto di Matematica Computazionale del CNR, Via Santa Maria 46, Pisa, Italy.
- GEORG, K. 1991. Approximation of integrals for boundary element methods. *SIAM J. Sci. Stat. Comput.* 12, 2, 443–453.
- GREENBAUM, A., GREENGARD, L., AND MCFADDEN, G. B. 1993. Laplace's equation and Dirichlet-Neumann map in multiply connected domains. *J. Comput. Phys.* 105, 267–278.
- GREENGARD, L. F. 1988. *The Rapid Evaluation of Potential Fields in Particle Systems*. The MIT Press, Cambridge, Mass.
- GREENGARD, L., AND ROKHLIN, V. 1987. A fast algorithm for particle simulations. *J. Comput. Phys.* 73, 325–438.
- GUERMOND, J. 1992. Numerical quadrature for layer potentials over curved domains in  $\mathbb{R}^3$ . *SIAM J. Numer. Anal.* 29, 1347–1369.
- HACKBUSCH, W., LAGE, C., AND SAUTER, S. A. 1995. On the efficient realization of sparse matrix techniques for integral equations with focus on panel clustering, cubature and software design aspects. Tech. Rep. 95-4. Berichtreihe des Mathematischen Seminars Christian-Albrechts-Universität zu Kiel Ludewig-Meyn-Str. D-24098, Kiel, Germany.
- HACKBUSCH, W., AND SAUTER, S. A. 1993. On the efficient use of the Galerkin-method to solve Fredholm integral equations. *Appl. Math.* 38, 301–322.
- JACKSON, J. 1975. *Classical Electrodynamics*. Wiley, New York.
- KEAST, P., AND FAIRWEATHER, G., EDS. 1997. *Numerical Integration: Recent Developments, Software, and Applications*. NATO ASI Series, vol. 203. Kluwer Academic Publishers, London, England.
- LANDAU, L. D., AND LIFSHITZ, E. M. 1980. *The Classical Theory of Fields*. Pergamon Press, Oxford, England.
- LYNESS, J. N. 1976. An error functional expansion for  $N$ -dimensional quadrature with an integrand function singular at a point. *Math. Comput.* 30, 133, 1–23.
- LYNESS, J. N. 1978. Quadrature over a simplex. II. A representation for the error functional. *SIAM J. Numer. Anal.* 15, 5, 870–887.
- LYNESS, J. N., AND COOLS, R. 1994. A survey of numerical cubature over triangles. In *Proceedings of Symposia in Applied Mathematics*, vol. 48. American Mathematical Society, Providence, R. I., pp. 127–150.
- LYNESS, J. N., AND MONEGATO, G. 1980. Quadrature error functional expansions for the simplex when the integrated function has singularities at vertices. *Math. Comput.* 34, 149, 213–225.
- MAYO, A. 1992. The rapid evaluation of integrals of potential theory on general region. *J. Comput. Phys.* 100, 236–245.
- MCKENNEY, A., GREENGARD, L., AND MAYO, A. 1995. A fast Poisson solver for complex geometries. *J. Comput. Phys.* 188, 348–355.
- NIEDERREITER, H. 1992. Random number generation and quasi-Monte Carlo methods. In *CBMS-NSF Regional Conference Series in Applied Mathematics*, vol. 63. SIAM, Philadelphia, Pa.
- PAN, V. Y., REIF, J. H., AND TATE, S. R. 1992. The power of combining the techniques of algebraic and numerical computing: Improved approximate multipoint polynomial evaluation and improved



- multipole algorithms. In *Proceedings of the 33rd Annual Symposium on Foundations of Computer Science*. IEEE Computer Science Press, Los Alamitos, Calif., pp. 703–713.
- PELLEGRINI, M. 1996. Electrostatic fields without singularities: Theory and algorithms. In *Proceedings of the 7th ACM-SIAM Symposium on Discrete Algorithms* (Atlanta, Ga., Jan. 28–30). ACM, New York, pp. 184–191. (Extended version in Tech. Rep. IMC B4-96-02, Istituto di Matematica Computazionale del CNR, Via Santa Maria 46, Pisa, Italy, pp. 184–191.)
- PELLEGRINI, M. 1997. Monte Carlo approximation of form factors with error bounded a priori. *Disc. Comput. Geom.* 17, 319–337.
- ROKHLIN, V. 1983. Rapid solution of integral equations of classical potential theory. *J. Comput. Phys.* 60, 187–207.
- SANTALO, L. A. 1976. *Integral Geometry and Geometric Probability*. Addison-Wesley, Reading, Mass.
- SAUTER, S. A., AND KRAPP, A. 1996. On the effect of numerical integration in the Galerkin boundary element method. *Numer. Mate.* 74, 337–359.
- SAUTER, S. A., AND SCHWAB, C. 1997. Quadrature for hp-Galerkin BEM in 3-D. *Numer. Mate.* 78, 2, 211–258.
- SCHWAB, C. 1994a. On numerical cubature of nearly singular surface integrals arising in BEM collocation. *Computing* 52, 139–159.
- SCHWAB, C. 1994b. Variable order composite quadrature of singular and nearly singular integrals. *Computing* 53, 173–194.
- SCHWAB, C. 1995. Boundary layer resolution in hierarchical plate modelling. *Math. Meth. Appl. Sci.* 18, 345–370.
- SCHWAB, C., AND WEDLAND, W. L. 1992a. Kernel properties and representation of boundary integral operators. *Math. Nachr.* 156, 187–216.
- SCHWAB, C., AND WEDLAND, W. L. 1992b. On numerical cubature of singular surface integrals on boundary element methods. *Num. Math.* 62, 343–369.
- STROUD, A. H. 1971. *Approximate calculation of multidimensional integrals*. Prentice-Hall, Englewood Cliffs, N. J.
- VON PETERSDORFF, T., AND SCHWAB, C. 1996. Fully discrete multiscale Galerkin BEM. Tech. Rep. TR-95-08. Seminar for Applied Mathematics, Dept. Mathematics, ETH, Zurich, Switzerland.
- ZHAO, F. 1987. An  $O(N)$  algorithm for three-dimensional N-body simulations. Tech. Rep. AITR-995. Artificial Intelligence Laboratory, MIT, Cambridge, Mass.
- ZHOU, P. B. 1993. *Numerical Analysis of Electromagnetic Fields*. Springer-Verlag, New York.

RECEIVED APRIL 1996; REVISED JUNE 1998; ACCEPTED JULY 1998